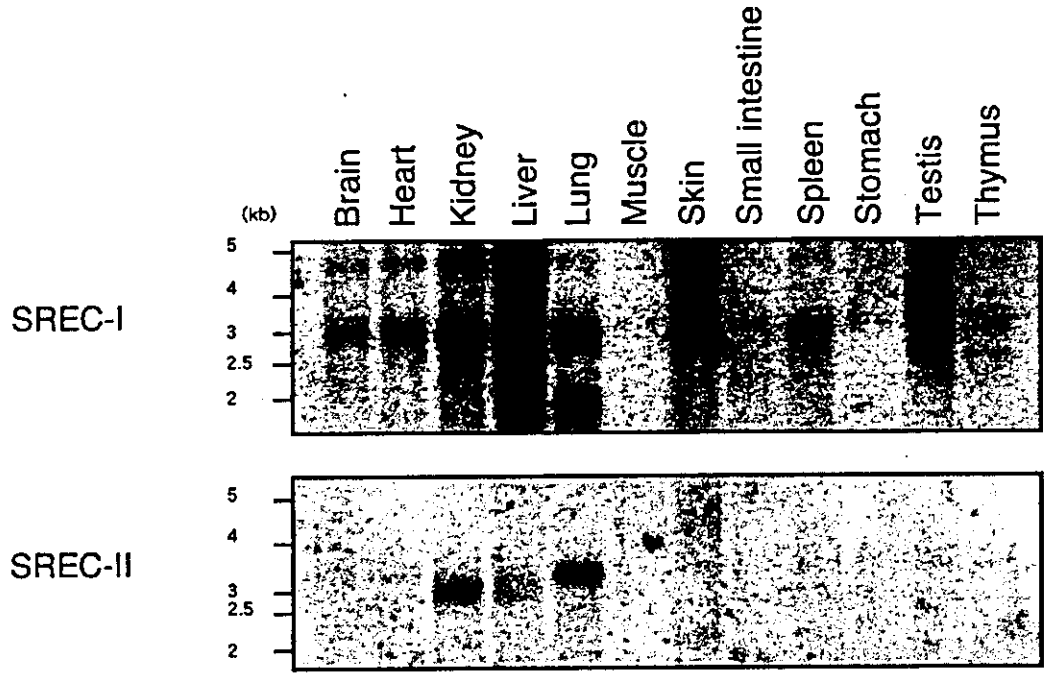

FIG. 1. **Northern blot analysis of SREC-I (*upper panel*) and SREC-II (*lower panel*) in various organs of a mouse.** Two micrograms of poly(A)$^+$ RNA was subjected to Northern blot analysis.

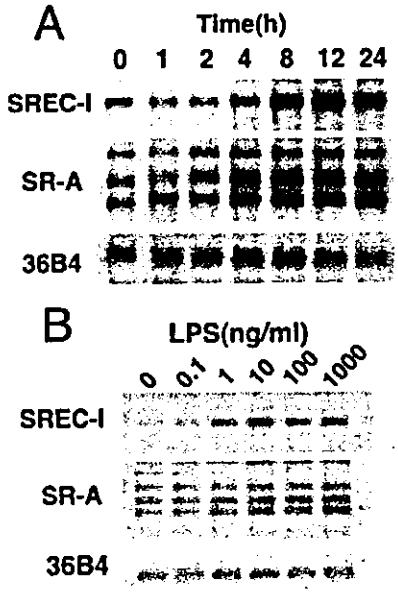

FIG. 2. **Northern blot analysis of SREC-I and SR-A in macrophages treated with LPS.** *A*, thioglycolate-elicited macrophages from C57BL/6 wild-type mice were treated with 100 ng/ml LPS for the indicated times. *B*, cells were treated with the indicated concentrations of LPS for 12 h. Two micrograms of poly(A)$^+$ RNA was subjected to Northern blot analysis. 36B4 was used as a loading control.

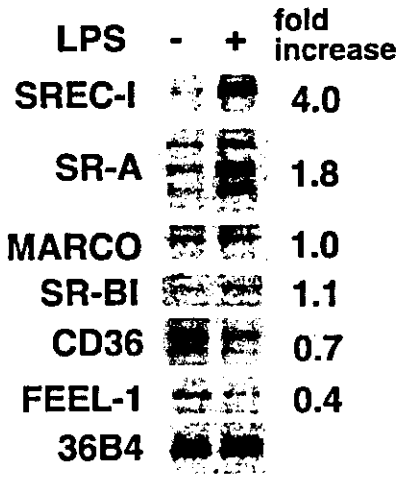

FIG. 3. **Northern blot analysis of scavenger receptors for Ac-LDL in macrophages treated with or without LPS.** Thioglycolate-elicited macrophages from C57BL/6 wild-type mice were treated with (+) or without (−) 100 ng/ml LPS for 12 h. Two micrograms of poly(A)$^+$ RNA was subjected to Northern blot analysis. Probes used were SREC-I, SR-A, MARCO, CD36, SR-BI, and FEEL-1. Signal intensity was corrected against the intensity of 36B4, and the relative signal increase ratio was calculated.

Generation of Mice Lacking the SREC-I and/or SR-A Gene—The intercross of the progeny (*SREC-I*$^{+/-}$) resulted in offspring of both sexes with all three genotypes at the SREC locus with the expected Mendelian ratios (105:191:85 $\chi^2 = 1.06$, $p > 0.05$) (Fig. 5*B*). Fig. 5*C* shows the results of Northern blot analyses of SREC-I in peritoneal macrophages. When hybridized with Probe A, which contains nearly the whole coding region of the SREC-I cDNA, Northern blot revealed a band with mRNA size of 2.9 kb in wild-type macrophages and a band of 2.4 kb in *SREC-I*$^{-/-}$ macrophages. When hybridized with Probe B, which contains the transmembrane domain, no band was detectable in *SREC-I*$^{-/-}$ macrophages. These results indicate that *SREC-I*$^{-/-}$ mice express a truncated transcript that lacks the transmembrane domain. *SREC-I*$^{-/-}$ mice were fertile and apparently normal. There were no significant differences in the growth curves of wild-type and *SREC-I*$^{-/-}$ mice. As shown in Table I, plasma levels of glucose, cholesterol, and triglycerides were not different between wild-type and *SREC-I*$^{-/-}$ mice. We failed to detect any pathological findings in the brain, lung, heart, liver, kidney, and testis of *SREC-I*$^{-/-}$ mice.

Northern blot analysis of four types of mice confirmed the absence of the expression of SR-A in both *SR-A*$^{-/-}$;*SREC-I*$^{+/+}$ and *SR-A*$^{-/-}$;*SREC-I*$^{-/-}$ mice as well as the expression of the disrupted allele of SREC-I in both *SR-A*$^{+/+}$;*SREC-I*$^{-/-}$ and *SR-A*$^{-/-}$;*SREC-I*$^{-/-}$ mice (Fig. 6*A*). Western blot analysis confirmed the absence of SREC-I protein (~140 and160 kDa) in both *SR-A*$^{+/+}$; *SREC-I*$^{-/-}$ and *SR-A*$^{-/-}$;*SREC-I*$^{-/-}$ mice (Fig. 6*B*).

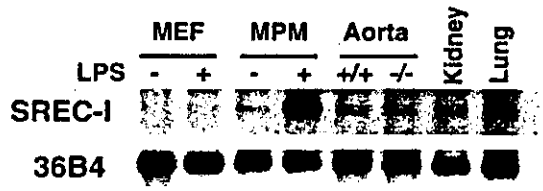

FIG. 4. **Northern blot analysis of SREC-I in normal and atherosclerotic aortas.** RNA were extracted from the following cells or organs: mouse embryonic fibroblasts (*MEF*) treated with (+) or without (−) 100 ng/ml LPS for 12 h; mouse peritoneal macrophages (*MPM*) treated with or without 100 ng/ml LPS for 12 h; kidney; lung; normal aortas from wild-type mice (*Aorta* +/+); and atherosclerotic aortas from apoE−/− mice (*Aorta* −/−). Aortic arches and the thoracic part of descending aortas with rampant visible plaques were excised from five 12-month-old mice. After adipose tissues surrounding the aortas were removed as much as possible, the aortas were used for the preparation of RNA. Three micrograms of poly(A)$^+$ RNA was subjected to Northern blot analysis of SREC-I. 36B4 was used as a loading control.

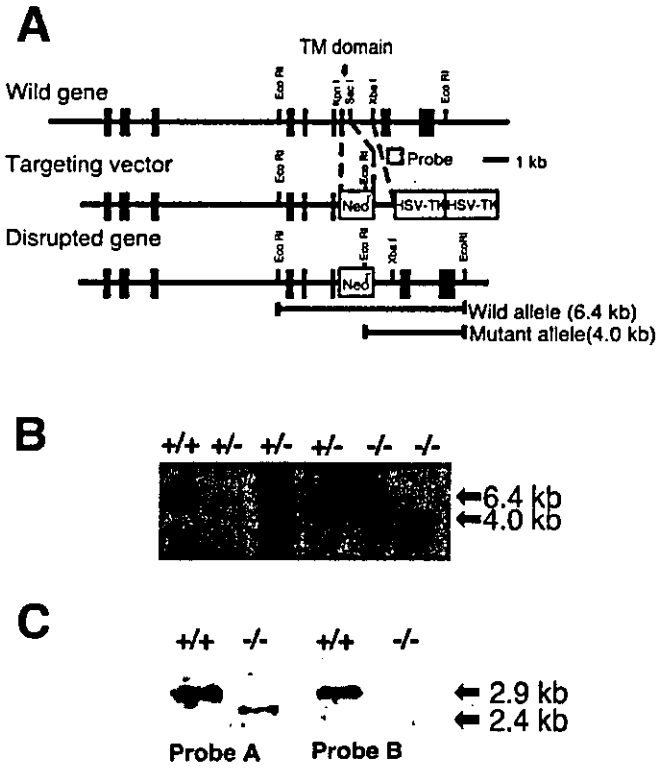

FIG. 5. **Targeted disruption of SREC-I gene.** *A*, map of the SREC-I gene and targeting construct. *Long boxes* represent exons. The exon coding transmembrane domain was replaced with the neomycin resistance gene (*Neo*^{r}) of targeting vector, which has a herpes simplex virus thymidine kinase (*HSV-TK*) cassette for a negative selection downstream of its short arm. A 0.5-kb fragment was used as a probe for Southern blot analysis (*shaded box*). *B*, Southern blot analysis. After digestion with EcoRI, tail DNA was used for Southern blot analysis. The size of the disrupted allele, 4 kb, was smaller than that of wild-type allele (6.4 kb). *C*, mRNA expression of SREC-I in peritoneal macrophage. Two micrograms of poly(A)$^+$ RNA from wild-type (+/+) and *SREC-I*$^{-/-}$ mice (−/−) macrophage was hybridized with two cDNA probes, namely Probe A, a 5′ 2-kb fragment spanning the extracellular and intracellular domains, and Probe B, a 0.1-kb fragment consisting of only the transmembrane domain.

LPS Stimulates Protein Expression of SREC-I—LPS significantly increased the SREC-I protein by ~2-fold in wild-type and *SR-A*$^{-/-}$;*SREC-I*$^{+/+}$ macrophages (Fig. 6*B*).

LPS Increases the Contribution of SREC-I to the Cellular Uptake and Degradation of the ^{125}I-Ac-LDL—In non-stimulated conditions (Fig. 7*A*) there was no significant difference in the specific uptake and degradation of ^{125}I-Ac-LDL between wild-type and *SR-A*$^{+/+}$;*SREC-I*$^{-/-}$ macrophages. Based on the values for 20 μg/ml degraded ^{125}I-Ac-LDL, *SR-A*$^{-/-}$;*SREC-I*$^{+/+}$ macrophages degraded significantly smaller amounts of ^{125}I-Ac-LDL (15%) than did wild-type macrophages, supporting the dominant role of SR-A in the uptake and degradation of ^{125}I-Ac-LDL in macrophages. Compared with *SR-A*$^{-/-}$;*SREC-I*$^{+/+}$ macrophages, *SR-A*$^{-/-}$;*SREC-I*$^{-/-}$ macrophages showed a further reduction in the specific uptake (21%) and degradation of ^{125}I-Ac-LDL (31%). Based on the values for 20 μg/ml degraded ^{125}I-Ac-LDL, the contribution of SR-A and SREC-I to the overall degradation of Ac-LDL was calculated to be 85 and 5%, respectively, in the non-stimulated condition.

LPS increased the uptake and degradation of Ac-LDL by 1.8-fold (Fig. 7*B*). In this condition, there was no significant difference in the specific uptake and degradation of ^{125}I-Ac-LDL between wild-type and *SR-A*$^{+/+}$;*SREC-I*$^{-/-}$ macrophages. Based on the values for 20 μg/ml degraded ^{125}I-Ac-LDL,

TABLE I

Plasma levels of glucose, total cholesterol, and triglycerides

After a 12-h fast, blood was collected from the retro-orbital venous plexus of mice aged 8 weeks. Plasma glucose, total cholesterol, and triglycerides were measured. All values are expressed as means ± S.E. No significant deference between wild-type and *SREC-I*$^{-/-}$ mice.

	Wild-type (+/+)	*SREC-I*$^{-/-}$
	mg/dl	
Glucose	61.1 ± 3.2 (n = 31)	63.2 ± 3.2 (n = 31)
Total cholesterol	89.7 ± 5.1 (n = 22)	82.0 ± 3.3 (n = 27)
Triglycerides	89.6 ± 9.4 (n = 22)	97.4 ± 10.3 (n = 27)

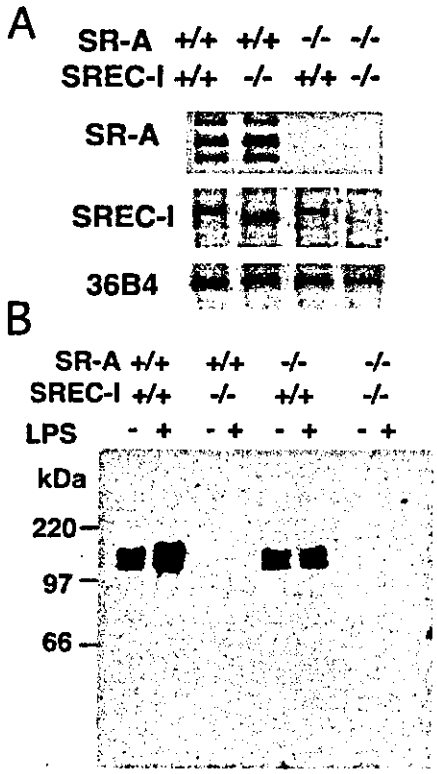

FIG. 6. **Expression of SR-A and SREC-I in macrophages isolated from wild-type, *SR-A*$^{+/+}$;*SREC-I*$^{-/-}$, *SR-A*$^{-/-}$;*SREC-I*$^{+/+}$, and *SR-A*$^{-/-}$;*SREC-I*$^{-/-}$ mice.** Thioglycolate-elicited peritoneal macrophages were prepared from wild-type, *SR-A*$^{+/+}$;*SREC-I*$^{-/-}$, *SR-A*$^{-/-}$;*SREC-I*$^{+/+}$, and *SR-A*$^{-/-}$;*SREC-I*$^{-/-}$ mice. *A*, Northern blot analysis of SR-A and SREC-I. One microgram of poly(A)$^+$ RNA from macrophages was hybridized with SR-A and SREC-I probes (Probe A). *B*, Western blot analysis of SREC-I in macrophages treated with or without LPS. After stimulation with (+) or without (−) 100 ng/ml LPS for 12 h, the cells were lysed with 0.1% SDS, and 50 μg of protein was subjected to SDS-PAGE. Immunoblotting was performed using the rat anti-mouse SREC-I antibody and an enhanced chemiluminescence kit.

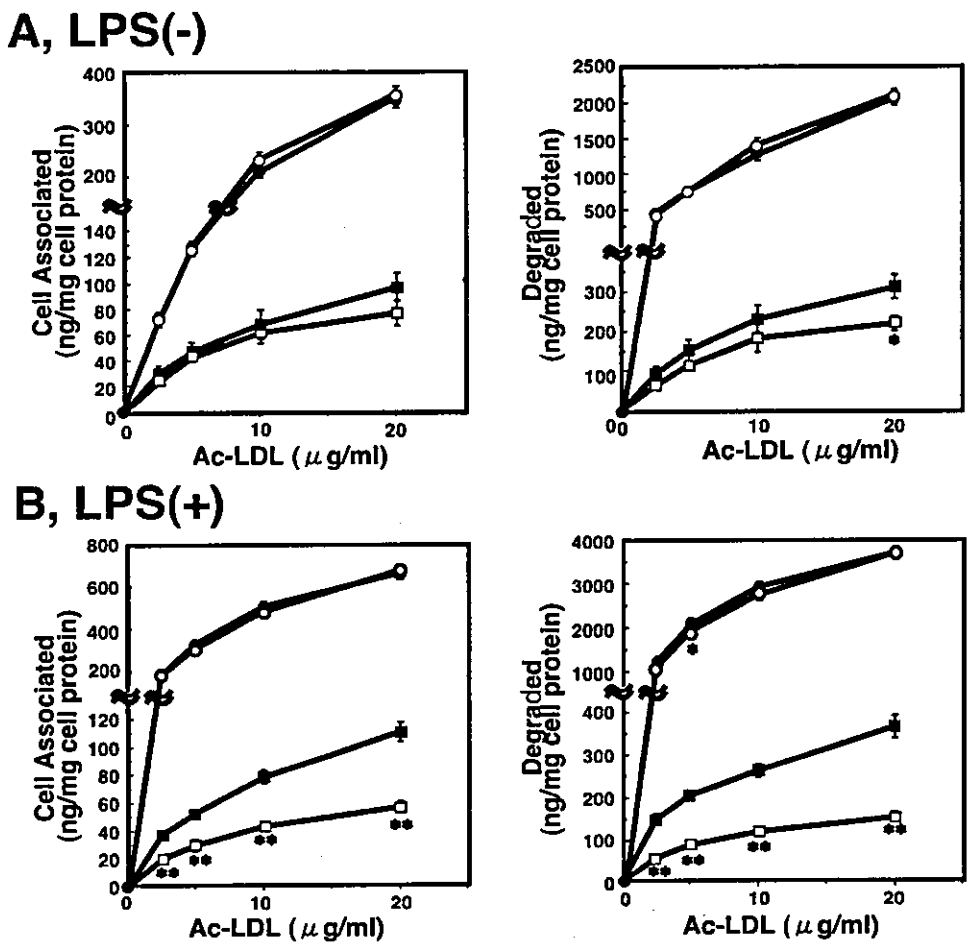

FIG. 7. **Cell association and degradation of ^{125}I-Ac-LDL by peritoneal macrophages isolated from wild-type, *SR-A*$^{+/+}$;*SREC-I*$^{-/-}$, *SR-A*$^{-/-}$;*SREC-I*$^{+/+}$, and *SR-A*$^{-/-}$;*SREC-I*$^{-/-}$ mice.** Thioglycolate-elicited peritoneal macrophages were prepared from four types of mice (n = 5), namely wild-type (*solid circle*), *SR-A*$^{+/+}$;*SREC-I*$^{-}$ (*open circle*), *SR-A*$^{-/-}$;*SREC-I*$^{+/+}$ (*solid square*), and *SR-A*$^{-/-}$;*SREC-I*$^{-/-}$ (*open square*). After treatment with (*panel B*) or without (*panel A*) 100 ng/ml LPS for 12 h, the cells were incubated with the indicated concentrations of ^{125}I-Ac-LDL with or without a 50-fold excess of unlabeled Ac-LDL at 37 °C. After 5 h, the amounts of ^{125}I-Ac-LDL associated or degraded were determined. Specific values were calculated by subtracting the nonspecific values from the total values. All values are expressed as means ± S.E. of five mice. *, $p < 0.05$ *versus* *SR-A*$^{-/-}$;*SREC-I*$^{+/+}$ mice; **, $p < 0.01$ *versus* *SR-A*$^{-/-}$; *SREC-I*$^{+/+}$ mice.

SR-A$^{-/-}$;*SREC-I*$^{+/+}$ macrophages degraded significantly smaller amounts of ^{125}I-Ac-LDL (10%) than did wild-type macrophages. Compared with *SR-A*$^{-/-}$;*SREC-I*$^{+/+}$ macrophages, *SR-A*$^{-/-}$;*SREC-I*$^{-/-}$ macrophages showed a further reduction in the specific uptake (49%) and degradation of ^{125}I-Ac-LDL (59%). Based on the values for 20 μg/ml degraded Ac-LDL, the contribution of SR-A and SREC-I to the overall degradation of ^{125}I-Ac-LDL was calculated to be 90 and 6%, respectively. LPS increased the absolute contribution of SR-A and SREC-I by 1.9- and 2.3-fold, respectively. On the other hand, LPS decreased the absolute contribution of other pathways by 31%.

DISCUSSION

In the present study, we have first shown that SREC-I, a novel member of the scavenger receptor family that recognizes modified lipoproteins, is expressed in a wide variety of tissues including macrophages and aortas, implicating its involvement in the development of atherosclerosis. The expression of SREC-I was not significantly different between normal and atherosclerotic aortas, although it was robustly induced by LPS in macrophages, a major cell type that is present in foam cell lesions. To define the precise role of SREC-I, we have generated wild-type, *SR-A*$^{+/+}$;*SREC-I*$^{-/-}$, *SR-A*$^{-/-}$;*SREC-I*$^{+/+}$, and *SR-A*$^{-/-}$;*SREC-I*$^{-/-}$ mice and compared the uptake and degradation of Ac-LDL in macrophages between these mice. Results show that the contribution of SREC-I to the overall uptake and degradation of Ac-LDL was 5% in the non-stimulated condition and 6% in the LPS-stimulated condition. Although the involvement of SREC-I was relatively small compared with that of SR-A, LPS increased the SREC-I mediated degradation by 2.3-fold, which accounted for 60% of the amounts of Ac-LDL degraded by the pathway independent of SR-A.

Because the responses of scavenger receptors to LPS are variable, we did not expect that LPS induced the expression of SREC-I in macrophages. LPS induces SR-A expression in mouse macrophages, which was confirmed in our experiments (Figs. 2 and 3) but not in THP-1 monocyte/macrophages (24) and human monocyte-derived macrophages (25). Because SR-A is able to bind LPS (26), the induction of SR-A by LPS may have a protective role against endotoxemia. This notion is in line with the susceptibility of SR-A knock-out mice to endotoxin shock (4, 27, 28). On the other hand, LPS down-regulates SR-B1 expression (29), which was confirmed in our experiments (Fig. 2).

The mechanism by which LPS induces SREC-I is intriguing. It is well known that LPS modulates gene expression though the activation of NF-κB signaling (30), and some of the effects are mediated by proinflammatory cytokines, whose expression is stimulated by LPS. However, there is no NF-κB binding site in the 5′-flanking region of the human SREC-I gene 1 kb upstream of the transcription initiation site (31). Furthermore,

LPS did not induce SREC-I expression in human umbilical vein endothelial cells, and tumor necrosis factor-α did not have increasing effects on SREC-I expression in mouse macrophages (data not shown). Further studies are warranted to decipher how LPS induces SREC-I expression.

Although SREC-I is expressed in macrophages, particularly when stimulated with LPS, there was no significant difference in the expression levels between normal and atherosclerotic aortas (Fig. 4). This suggests that other cell types such as endothelial cells and smooth muscle cells in the aortas express comparable levels of SREC-I.

SR-A is the major pathway for the uptake and degradation of Ac-LDL, accounting for 80% of the total activity (4, 5). Because other scavengers are expressed in macrophages (Fig. 2) and are able to bind Ac-LDL (2), the question is which scavenger receptor is the second most important in the uptake and degradation of Ac-LDL. Our results have revealed that the role of SREC-I is relatively minor in the non-stimulated macrophages, which is largely consistent with the recent report by Kunjathoor *et al.* (22). According to them, SR-A and CD36 account for 75–90% of the total amounts of chemically modified LDL degraded by macrophages. In SR-A-deficient macrophages stimulated with LPS, however, the absolute contribution of SREC-I was significantly increased by 2.3-fold, accounting for 60% of the SR-A-independent uptake and degradation of Ac-LDL (Fig. 7*B*). The degree of increase in the SREC-I mediated uptake and degradation of Ac-LDL is largely comparable with that in SREC-I protein expression (Fig. 6*B*). It is interesting to note that LPS decreased the absolute contribution of the other endocytic pathway, which is independent of either SR-A or SREC-I, by 31%. This finding is consistent with the Northern blot results that show that LPS did not significantly increase the expression of the other members of scavenger receptor family such as MARCO, SR-BI, CD36, and FEEL-1 (Fig. 3). Thus, SREC-I is the second most important receptor mediating the uptake of Ac-LDL, at least in macrophages stimulated with LPS. Given the activated state of macrophages in rupture-prone unstable plaques (8), particularly in plaques infected with microorganisms such as *Chlamydia*, which is associated with an increased prevalence of coronary events (32), SREC-I may take a significant part in the foam cell formation in these pathological conditions. Other aspects of LPS may be involved in the atherogenesis. For example, Baranova *et al.* (29) and Khovidhunkit *et al.* (33) have recently reported that LPS inhibits high density lipoprotein-mediated cholesterol efflux via down-regulation of the expression of ABCA1 and ABCG1. These observations are consistent not only with the ability of LPS to stimulate lipid accumulation in macrophages *in vitro* (34) but also with the proatherogenic effects of LPS (9) and its cognate receptor, Toll-like receptor 4, *in vivo* (11).

Functions of adhesion molecules have been assigned to both SR-A and SREC-I/II. Chinese hamster ovary cells overexpressing SR-A have an increased ability to adhere to plastic surfaces (35). Likewise, intense aggregation was observed when SREC-I-expressing fibroblast L-cells were mixed with those expressing SREC-II (7). Thus, it is reasonable to speculate that *SREC-I*$^{-/-}$ mice have some phenotypes with regard to cell adhesion. However, there were no obvious abnormalities in the pathologies (data not shown).

The precise roles of scavenger receptors in atherogenesis have been tested only for SR-A and CD36. With regard to SR-A, we (4, 36, 37) and Babaev *et al.* (38) have reported that SR-A deficiency protects against the development of atherosclerosis in either apoE, LDL receptor-deficient, or wild-type mice. de Winther *et al.* (39), however, recently reported apparently opposite results, *i.e.* SR-A deficiency leads to more complex lesions in the APOE3Leiden mice. The same group reported the reduction in atherosclerosis in LDL receptor knock-out mice in which SR-A was overexpressed in a macrophage-specific manner (40). These contradictory results could be attributed to the broad repertoire of functions and the widespread expression of SR-A (41). With regard to CD36, Febbraio *et al.* have reported that CD36 deficiency protects against atherosclerosis in an apoE-deficient background (42). Availability of the *SR-A*$^{-/-}$; *SREC-I*$^{-/-}$ mice should allow us to determine the role of SREC-I in the development of atherosclerosis by crossing with the genetically hyperlipidemic mice, for example. If the hypothesis is correct, SREC-I should be a new target for preventing atherosclerosis.

Acknowledgments—We thank Kimiko Saito, Megumi Herai, Mihoko Kusubae, and Rie Tamura for excellent technical assistance. We also thank Tetsuya Kitamine, Stephane Perrey, Michiyo Amemiya-Kudo, and Takanari Gotoda for helpful comments and discussion.

REFERENCES

1. Brown, M. S., and Goldstein, J. L. (1983) *Annu. Rev. Biochem.* **52,** 223–261
2. Krieger, M. (1997) *Curr. Opin. Lipidol.* **8,** 275–280
3. Kodama, T., Freeman, M., Rohrer, L., Zabrecky, J., Matsudaira, P., and Krieger, M. (1990) *Nature* **343,** 531–535
4. Suzuki, H., Kurihara, Y., Takeya, M., Kamada, N., Kataoka, M., Jishage, K., Ueda, O., Sakaguchi, H., Higashi, T., Suzuki, T., Takashima, Y., Kawabe, Y., Cynshi, O., Wada, Y., Honda, M., Kurihara, H., Aburatani, H., Doi, T., Matsumoto, A., Azuma, S., Noda, T., Toyoda, Y., Itakura, H., Yazaki, Y., Horiuchi, S., Takahashi, K., Kruijt, J. K., Van Berkel, T. J. C., Steinbrecher, U. P., Ishibashi, S., Maeda, N., Gordon, S., and Kodama, T. (1997) *Nature* **386,** 292–296
5. Lougheed, M., Lum, C. M., Ling, W., Suzuki, H., Kodama, T., and Steinbrecher, U. (1997) *J. Biol. Chem.* **272,** 12938–12944
6. Adachi, H., Tsujimoto, M., Arai, H., and Inoue, K. (1997) *J. Biol. Chem.* **272,** 31217–31220
7. Ishii, J., Adachi, H., Aoki, J., Koizumi, H., Tomita, S., Suzuki, T., Tsujimoto, M., Inoue, K., and Arai, H. (2002) *J. Biol. Chem.* **277,** 39696–39702
8. Libby, P. (2002) *Nature* **420,** 868–874
9. Lehr, H. A., Sagban, T. A., Ihling, C., Zahringer, U., Hungerer, K. D., Blumrich, M., Reifenberg, K., and Bhakdi, S. (2001) *Circulation* **104,** 914–920
10. Lynn, W. A., and Cohen, J. (1995) *Clin. Infect. Dis.* **20,** 143–158
11. Vink, A., Schoneveld, A. H., van der Meer, J. J., van Middelaar, B. J., Sluijter, J. P., Smeets, M. B., Quax, P. H., Lim, S. K., Borst, C., Pasterkamp, G., and de Kleijn, D. P. (2002) *Circulation* **106,** 1985–1990
12. Sambrook, J., and Russell, D. W. (2001) *Molecular Cloning: A Laboratory Manual*, Cold Spring Harbor Laboratory Press, Cold Spring Harbor, NY
13. Zhang, S. H., Reddick, R. L., Piedrahita, J. A., and Maeda, N. (1992) *Science* **258,** 468–471
14. Yagyu, H., Kitamine, T., Osuga, J., Tozawa, R., Chen, Z., Kaji, Y., Oka, T., Perrey, S., Tamura, Y., Ohashi, K., Okazaki, H., Yahagi, N., Shionoiri, F., Iizuka, Y., Harada, K., Shimano, H., Yamashita, H., Gotoda, T., Yamada, N., and Ishibashi, S. (2000) *J. Biol. Chem.* **275,** 21324–21330
15. Okazaki, H., Osuga, J., Tamura, Y., Yahagi, N., Tomita, S., Shionoiri, F., Iizuka, Y., Ohashi, K., Harada, K., Kimura, S., Gotoda, T., Shimano, H., Yamada, N., and Ishibashi, S. (2002) *Diabetes* **51,** 3368–3375
16. Tamura, Y., Adachi, H., Osuga, J., Ohashi, K., Yahagi, N., Sekiya, M., Okazaki, H., Tomita, S., Iizuka, Y., Shimano, H., Nagai, R., Kimura, S., Tsujimoto, M., and Ishibashi, S. (2003) *J. Biol. Chem.* **278,** 12613–12617
17. Ishibashi, S., Brown, M. S., Goldstein, J. L., Gerard, R. D., Hammer, R. E., and Herz, J. (1993) *J. Clin. Investig.* **92,** 883–893
18. Goldstein, J. L., Basu, S. K., and Brown, M. S. (1983) *Methods Enzymol.* **98,** 241–260
19. Perrey, S., Ishibashi, S., Kitamine, T., Osuga, J., Yagyu, H., Chen, Z., Shionoiri, F., Iizuka, Y., Yahagi, N., Tamura, Y., Ohashi, K., Harada, K., Gotoda, T., and Yamada, N. (2001) *Atherosclerosis* **154,** 51–60
20. Elomaa, O., Kangas, M., Sahlberg, C., Tuukkanen, J., Sormunen, R., Liakka, A., Thesleff, I., Kraal, G., and Tryggvason, K. (1995) *Cell* **80,** 603–609
21. Acton, S. L., Scherer, P. E., Lodish, H. F., and Krieger, M. (1994) *J. Biol. Chem.* **269,** 21003–21009
22. Kunjathoor, V. V., Febbraio, M., Podrez, E. A., Moore, K. J., Andersson, L., Koehn, S., Rhee, J. S., Silverstein, R., Hoff, H. F., and Freeman, M. W. (2002) *J. Biol. Chem.* **277,** 49982–49988
23. Adachi, H., and Tsujimoto, M. (2002) *J. Biol. Chem.* **277,** 34264–34270
24. Fitzgerald, M. L., Moore, K. J., Freeman, M. W., and Reed, G. L. (2000) *J. Immunol.* **164,** 2692–2700
25. van Lenten, B. J., and Fogelman, A. M. (1992) *J. Immunol.* **148,** 112–116
26. Hampton, R. Y., Golenbock, D. T., Penman, M., Krieger, M., and Raetz, C. R. (1991) *Nature* **352,** 342–344
27. Haworth, R., Platt, N., Keshav, S., Hughes, D., Darley, E., Suzuki, H., Kurihara, Y., Kodama, T., and Gordon, S. (1997) *J. Exp. Med.* **186,** 1431–1439
28. Ishiguro, T., Naito, M., Yamamoto, T., Hasegawa, G., Gejyo, F., Mitsuyama, M., Suzuki, H., and Kodama, T. (2001) *Am. J. Pathol.* **158,** 179–188
29. Baranova, I., Vishnyakova, T., Bocharov, A., Chen, Z., Remaley, A. T., Stonik, J., Eggerman, T. L., and Patterson, A. P. (2002) *Infect Immun.* **70,** 2995–3003
30. Muller, J. M., Ziegler-Heitbrock, H. W., and Baeuerle, P. A. (1993) *Immunobiology* **187,** 233–256

31. Adachi, H., and Tsujimoto, M. (2002) *J. Biol. Chem.* **277,** 24014–24021
32. Becker, A. E., de Boer, O. J., and van Der Wal, A. C. (2001) *Annu. Rev. Med.* **52,** 289–297
33. Khovidhunkit, W., Moser, A. H., Shigenaga, J. K., Grunfeld, C., and Feingold, K. R. (2001) *J. Lipid Res.* **42,** 1636–1644
34. Funk, J. L., Feingold, K. R., Moser, A. H., and Grunfeld, C. (1993) *Atherosclerosis* **98,** 67–82
35. Fraser, I., Hughes, D., and Gordon, S. (1993) *Nature* **364,** 343–346
36. Sakaguchi, H., Takeya, M., Suzuki, H., Hakamata, H., Kodama, T., Horiuchi, S., Gordon, S., van der Laan, L. J., Kraal, G., Ishibashi, S., Kitamura, N., and Takahashi, K. (1998) *Lab. Investig.* **78,** 423–434
37. Kamada, N., Kodama, T., and Suzuki, H. (2001) *J. Atheroscler. Thromb.* **8,** 1–6
38. Babaev, V. R., Gleaves, L. A., Carter, K. J., Suzuki, H., Kodama, T., Fazio, S., and Linton, M. F. (2000) *Arterioscler. Thromb. Vasc. Biol.* **20,** 2593–2599
39. de Winther, M. P., Gijbels, M. J., van Dijk, K. W., van Gorp, P. J., Suzuki, H., Kodama, T., Frants, R. R., Havekes, L. M., and Hofker, M. H. (1999) *Atherosclerosis* **144,** 315–321
40. de Winther, M. P., Gijbels, M. J., van Dijk, K. W., Havekes, L. M., and Hofker, M. H. (2000) *Int. J. Tissue React.* **22,** 85–91
41. Platt, N., and Gordon, S. (2001) *J. Clin. Investig.* **108,** 649–654
42. Febbraio, M., Podrez, E. A., Smith, J. D., Hajjar, D. P., Hazen, S. L., Hoff, H. F., Sharma, K., and Silverstein, R. L. (2000) *J. Clin. Investig.* **105,** 1049–1056

THE JOURNAL OF BIOLOGICAL CHEMISTRY

Vol. 279, No. 50, Issue of December 10, pp. 52425–52436, 2004
Printed in U.S.A.

Anti-apoptotic Actions of the Platelet-activating Factor Acetylhydrolase I α_2 Catalytic Subunit*

Received for publication, September 23, 2004
Published, JBC Papers in Press, September 28, 2004, DOI 10.1074/jbc.M410967200

Fanny Bonin‡§¶, Scott D. Ryan‡§, Lamiaa Migahed‡‖, Fan Mo‡‖, Jessica Lallier‡, Doug J. Franks, Hiroyuki Arai‡‡, and Steffany A. L. Bennett‡§§**

*From the ‡Neural Regeneration Laboratory, Department of Biochemistry, Microbiology, and Immunology and the **Department of Pathology, University of Ottawa, Ottawa, Ontario K1H 8M5, Canada and ‡‡Graduate School of Pharmaceutical Sciences, University of Tokyo, 3-1, Hongo-7, Bunkyo-ku, Tokyo 113-0033, Japan*

Platelet-activating factor (PAF) is an important mediator of cell loss following diverse pathophysiological challenges, but the manner in which PAF transduces death is not clear. Both PAF receptor-dependent and -independent pathways are implicated. In this study, we show that extracellular PAF can be internalized through PAF receptor-independent mechanisms and can initiate caspase-3-dependent apoptosis when cytosolic concentrations are elevated by ~15 pM/cell for 60 min. Reducing cytosolic PAF to less than 10 pM/cell terminates apoptotic signaling. By pharmacological inhibition of PAF acetylhydrolase I and II (PAF-AH) activity and down-regulation of PAF-AH I catalytic subunits by RNA interference, we show that the PAF receptor-independent death pathway is regulated by PAF-AH I and, to a lesser extent, by PAF-AH II. Moreover, the anti-apoptotic actions of PAF-AH I are subunit-specific. PAF-AH I α_1 regulates intracellular PAF concentrations under normal physiological conditions, but expression is not sufficient to reduce an acute rise in intracellular PAF levels. PAF-AH I α_2 expression is induced when cells are deprived of serum or exposed to apoptogenic PAF concentrations limiting the duration of pathological cytosolic PAF accumulation. To block PAF receptor-independent death pathway, we screened a panel of PAF antagonists (CV-3988, CV-6209, BN 52021, and FR 49175). BN 52021 and FR 49175 accelerated PAF hydrolysis and inhibited PAF-mediated caspase 3 activation. Both antagonists act indirectly to promote PAF-AH I α_2 homodimer activity by reducing PAF-AH I α_1 expression. These findings identify PAF-AH I α_2 as a potent anti-apoptotic protein and describe a new means of pharmacologically targeting PAF-AH I to inhibit PAF-mediated cell death.

Platelet-activating factor (PAF,[1] 1-*O*-alkyl-2-acetyl-*sn*-glycero-3-phosphocholine) is a key mediator of neuronal death in ischemia, encephalitis, epileptic seizure, meningitis, and human immunodeficiency virus-1 dementia *in vivo* and participates in etoposide-, prion-, and β-amyloid-induced cell death *in vitro* (1–7). In the periphery, pathological increases in PAF concentrations underlie cytotoxicity in chronic inflammatory dermatoses and lethality in systemic anaphylaxis (8, 9). Although the majority of PAF effects are understood to be transduced by its G-protein-coupled receptor (PAFR) (10), PAFR signaling has been shown to be both pro- and anti-apoptotic. Ectopic PAFR expression exacerbates cell death induced by etoposide and mitomycin C but protects cells from tumor necrosis factor α, TRAIL, and extracellular PAF (6, 7, 11, 12). These opposing effects likely depend upon the relative ratio of NF-κB-dependent pro- and anti-apoptotic gene products elicited in different cell types in response to the combination of an external apoptotic inducer and PAF (6).

Accumulating evidence points to additional PAF signaling pathways transduced independently of PAFR (11, 13–17). PAFR-negative cells undergo apoptosis when extracellular PAF concentrations reach 100 nM and necrosis when PAF levels exceed the critical micelle concentration of 3 μM (11). Little is known about how PAF signals cell death in the absence of PAFR. PAF activates NF-κB, glycogen synthase kinase 3β, and caspase 3 and triggers mitochondrial release of cytochrome *c* (6, 18–20). Whether or not these effects are dependent on PAFR activation is not clear.

One approach to intervening in both PAFR-dependent and -independent cell death lies in reducing pathological increases in PAF. PAF is hydrolyzed by a unique family of serine esterases or PAF acetylhydrolases (PAF-AHs) that cleave the biologically *sn*-2 active side chain generating *lyso*-PAF. Three PAF-AH enzymes have been identified. Cytosolic PAF-AH I cleaves the acetyl group at the *sn*-2 position of PAF and PAF-like lipids with other phosphate head groups (21). The enzymatic complex is a G-protein-like trimer composed of two 29-kDa α_1 and α_2 catalytic subunits. The α subunits form homodimers or heterodimers that complex with a noncatalytic 45-kDa regulatory β subunit, LIS1. Mutations in the *LIS1* gene

* This work was supported in part by grants from the Alzheimer Society of Canada, Alzheimer Society of Saskatchewan, and the Canadian Institute of Health Research Joint Initiative (to S. A. L. B.). The costs of publication of this article were defrayed in part by the payment of page charges. This article must therefore be hereby marked "*advertisement*" in accordance with 18 U.S.C. Section 1734 solely to indicate this fact.

The nucleotide sequence(s) reported in this paper has been submitted to the GenBank™/EBI Data Bank with accession number(s) AY225592.

§ Both authors contributed equally to this work.

¶ Supported by a graduate studentship from the Scottish Rite/Roher Foundation.

‖ Supported by a National Research Council undergraduate research award.

§§ Ontario Mental Health Foundation Intermediate Investigator and a Canadian Institute of Health Research New Investigator. To whom correspondence should be addressed: Neural Regeneration Laboratory, Dept. of Biochemistry, Microbiology, and Immunology, University of Ottawa, Ottawa, Ontario K1H 8M5, Canada. Tel.: 613-562-5600 (Ext. 8372); Fax: 613-562-5452; E-mail: sbennet@uottawa.ca.

[1] The abbreviations used are: PAF, platelet-activating factor; B-PAF, Bodipy-platelet-activating factor; B-*lyso*-PAF, Bodipy *lyso*-PAF; BSA, bovine serum albumin; GAPDH, glyceraldehyde-3-phosphate dehydrogenase; DFP, diisopropyl fluorophosphate; DTNB, 5,5prime-dithiobis(2-nitrobenzoic acid; mc-PAF, methyl-carbamyl platelet-activating factor; PAF-AH, PAF acetylhydrolase; PAFR, platelet-activating factor receptor; PARP, poly(ADP-ribose) polymerase; PBS, phosphate-buffered saline; siRNA, small interfering RNA; RT, reverse transcription; TUNEL, terminal deoxytransferase dUTP nick-end labeling; ANOVA, analysis of variance; EGFP, enhanced green fluorescent protein.

are the genetic determinant of Miller-Dieker syndrome, a developmental brain disorder defined by type 1 lissencephaly (22). PAF-AH II is a single 40-kDa polypeptide (23). This isoenzyme recognizes both PAF and acyl analogs of PAF with moderate length *sn*-2 chains as well as short chain diacylglycerols, triacylglycerols, and acetylated alkanols (24). Ectopic expression reduces cell death triggered by oxidative stress (25, 26). Plasma PAF-AH is a 45-kDa monomer secreted into circulation by endothelial and hematopoietic cells (27, 28). The enzyme recognizes PAF and PAF analogs with short to medium *sn*-2 chains including oxidatively cleaved long chain polyunsaturated acyl chains (24). *In vitro*, recombinant plasma PAF-AH or ectopic expression protects cells from excitotoxicity or hypercholesterolemia (29–31). *In vivo*, intravenous injection of human plasma PAF-AH reduces lethality in experimental models of anaphylactic shock (8). These findings provide compelling evidence that PAF-AH activity regulates PAF-mediated apoptosis. It remains to be determined whether these enzymes can, in fact, be targeted to inhibit PAF-mediated degeneration and disease.

In this study, we used the PC12 cell model to investigate the anti-apoptotic actions of PAF-AH I and PAF-AH II in the PAFR-independent death pathway. We show that PC12 cells express all three PAF-AH I proteins (α_1, α_2, and LIS1) as well as PAF-AH II but not plasma PAF-AH or PAFR. Expression of PAF-AH I α_2 but not PAF-AH I α_1 is induced when PC12 cells are deprived of serum. We found that this induction regulates the duration of apoptotic signaling initiated by PAF challenge. To enhance the endogenous anti-apoptotic activity of PAF-AH I α_2, we screened a panel of PAF antagonists, and we identified two compounds that blocked PAFR-independent death. Both compounds, the fungal derivative FR 49175 and the ginkgolide BN 52021, protected cells by accelerating PAF hydrolysis. Most surprisingly, both inhibitors suppressed α_1 protein expression thereby promoting α_2/α_2 homodimer activity following PAF treatment. These findings point to a novel anti-apoptotic function for the α_2 subunit of PAF-AH I and a potential means of pharmacologically targeting PAF-AH enzymes to reduce PAF-mediated cell death.

EXPERIMENTAL PROCEDURES

Cell Culture—PC12-AC cells, a clonal derivative of the PC12 pheochromocytoma cell line (American Tissue Culture Collection), were cultured in complete media composed of RPMI 1640 containing 10% horse serum and 5% newborn calf serum at 37 °C in a 5% CO_2, 95% air atmosphere. Culture reagents were obtained from Invitrogen.

Reverse Transcriptase (RT)-PCR—Rat brain RNA was prepared from Wistar rats ~3 months of age (Charles River Breeding Laboratories). Rodents were anesthetized with sodium pentobarbital and euthanized by decapitation. All manipulations were performed in compliance with approved institutional protocols and according to the strict ethical guidelines for animal experimentation established by the Canadian Council for Animal Care. Total RNA was isolated using Trizol reagent (Invitrogen) and treated with RQ1-DNase I (Promega) to eliminate residual genomic DNA. First strand cDNA synthesis was performed using random hexamer primers (Promega) and Superscript II RT (Invitrogen). Control reactions for residual genomic contamination were carried out in the absence of Superscript II RT. cDNA synthesis was performed using 5 units of *Taq* DNA polymerase (Invitrogen) in the presence of 1 mM $MgCl_2$ and 10 pmol per primer for glyceraldehyde phosphate dehydrogenase (GAPDH), 20 pmol per primer for PAF-AH II2, PAF-AH II3, and PAF-AH II4, and 25 pmol per primer for PAF-AH I α_1, PAF-AH I α_2, PAF-AH I LIS1, PAF-AH II1, plasma PAF-AH, and PAFR. Sequences are provided in Table I. Primers were synthesized at the Biochemistry Research Institute, University of Ottawa. Reactions were amplified in a GeneAmp PCR System 2400 (Applied Biosystems): 94 °C for 5 min, 30–35 cycles of 94 °C for 30 s, 55 °C for 60 s, and 72 °C for 2 min, followed by a final incubation at 72 °C for 7 min.

Western Analysis—Rat brain protein was prepared from Wistar rat pups on postnatal day 10. Rodents were anesthetized with sodium pentobarbital and euthanized by decapitation. Brains were removed and placed in a 10-cm tissue culture plate containing artificial cerebrospinal fluid (26 mM $NaHCO_3$, 124 mM NaCl, 5 mM KCl, 2 mM $CaCl_2$, 1.3 mM $MgCl_2$, 10 mM D-glucose, 100 units/ml penicillin, 100 μg/ml streptomycin, pH 7.3) and homogenized using a Tissue Tearor (Fisher). Protein was isolated using Trizol reagent (Invitrogen). Proteins from PC12 cells were isolated in RIPA buffer (10 mM PBS, 1% Nonidet P-40, 0.5% sodium deoxycholate, 0.1% SDS, 30 μl/ml aprotinin, 10 mM sodium orthovanadate, 100 μl/ml phenylmethylsulfonyl fluoride). Protein samples (30 μg) were separated by SDS-PAGE under reducing conditions. Antibodies were diluted in 1% heat-denaturated casein in 10 mM phosphate-buffered saline (PBS: 10 mM sodium phosphate, 2.7 mM KCl, 4.3 mM NaCl, pH 7.5). Western analyses were performed using polyclonal anti-LIS1 (1:500, Chemicon), monoclonal anti-α_1 (1:1000, Dr. H. Arai, University of Tokyo, Tokyo, Japan), monoclonal anti-α_2 (1:1000, Dr. H. Arai), poly(ADP-ribose) polymerase (PARP, 1:10, 000, Clontech), and actin (1:1000, Sigma). Secondary antibodies were horseradish peroxidase-conjugated or biotin-conjugated anti-mouse IgG (1:2000, Jackson ImmunoResearch; 1:10, 000, Sigma) or anti-rabbit IgG antibodies (1:5000, Jackson ImmunoResearch), and tertiary reagents were extravidin alkaline phosphatase (1:300,000, Sigma) as appropriate. Immunoreactive bands were visualized using SuperSignal West Pico (MJS BioLynx Inc.) or nitro blue tetrazolium/5-bromo-4-chloro-3-indolyl phosphate (Sigma). Densitometry was performed using ImageJ analysis software (National Institutes of Health) standardized to actin loading controls.

PAF-AH Activity—PAF-AH activities in complete media, serum-free RPMI, PC12-AC cells, PC12-AC conditioned treatment media, and C57Bl/6 mouse brain ~3 months of age (positive control) were determined using a commercial PAF-AH assay kit (Cayman Chemicals). Cells and tissue were homogenized in 250 mM sucrose, 10 mM Tris-HCl (pH 7.4), and 1 mM EDTA using a Tissue Tearor (Fisher). Samples were centrifuged at 600 × *g* for 10 min and at 100,000 × *g* for 60 min. Cytosolic supernatants were concentrated using an Amicon centrifuge concentrator with a molecular mass cut-off of 10,000 kDa (Millipore). Protein (30–50 μg) was incubated with C_{16}-2-thio-PAF substrate for 30 min at room temperature. In some cases, lysates were pretreated for 15 or 30 min at room temperature with diisopropyl fluorophosphate (DFP) at the concentrations indicated in the text. Percent inhibition was calculated relative to lysates treated with vehicle (PBS) for the same time. Hydrolysis of the thioester bond at the *sn*-2 position was detected by conjugation with 5,5′-dithiobis(2-nitrobenzoic acid) (DTNB) at 405 nM. Control reactions included samples incubated without lysate or media and samples incubated without substrate.

Internalization Assay (Live Cell Imaging)—PC12-AC cells (5 × 10^4 cells/well) were plated in complete media overnight in 24-well plates (VWR Scientific) coated with 0.1% gelatin. Cells were washed in 10 mM PBS and incubated with 1 μM Bodipy FL C_{11}-PAF (B-PAF) in RPMI 1640 containing 0.1% bovine serum albumin (BSA, Sigma). B-PAF was custom-synthesized for our laboratory by Molecular Probes. At each time point (0, 10, 20, 30, 40, 50, 60, 80, 90, 100, 110, and 120 min), incubation media were removed, and cells were washed with 10 mM PBS. Live cell imaging under phase and fluorescence of identical cell fields was performed using a DMR inverted microscope (Leica) equipped with a QICAM digital camera (Quorum Technologies) and captured using OpenLab software version 3.17 (Improvision). Following time-lapse imaging, the incubation media were replaced, and internalization was allowed to continue. Quantitation of fluorescence intensity of individual cells was performed using the Advanced Measurement Module of OpenLab version 3.17.

Lipid Extraction and TLC—PC12-AC cells seeded at 1 × 10^5 cells onto 10-cm plates were maintained in complete media at 37 °C in 5% CO_2 for 72 h. Cultures were incubated at 37 °C with 1 μM B-PAF in RPMI 1640 containing 0.1% BSA for 0, 5, 15, 30, 45, 60, and 75 min. At each time point, 4 plates/condition were removed from the incubator and were placed on ice. One ml of methanol acidified with 2% acetic acid was added to each plate, and the extracellular fraction was collected. This fraction contained B-PAF in the culture media and uninternalized B-PAF bound to cell surface proteins or associated with the plasma membrane. The remaining monolayer of cells was collected in acidified methanol by scraping the plate with a cell lifter (Fisher). Lipids were extracted from the extracellular milieu and cytosolic fractions by the Bligh and Dyer method (32) and developed on TLC plates (20 × 20 cm Silica Gel 60 (Fisher) in a solvent system of chloroform/methanol/acetic acid/water (50:30:8:5, v/v). B-PAF and B-*lyso*-PAF (Molecular Probes) were used as authentic markers. Fluorescent lipids were visualized under UV light using AlphaImager-1220 software (Alpha Innotech Corp.). Fluorescence intensity corresponding to lipid yield was determined by densitometry using the Advanced Measurement Module of

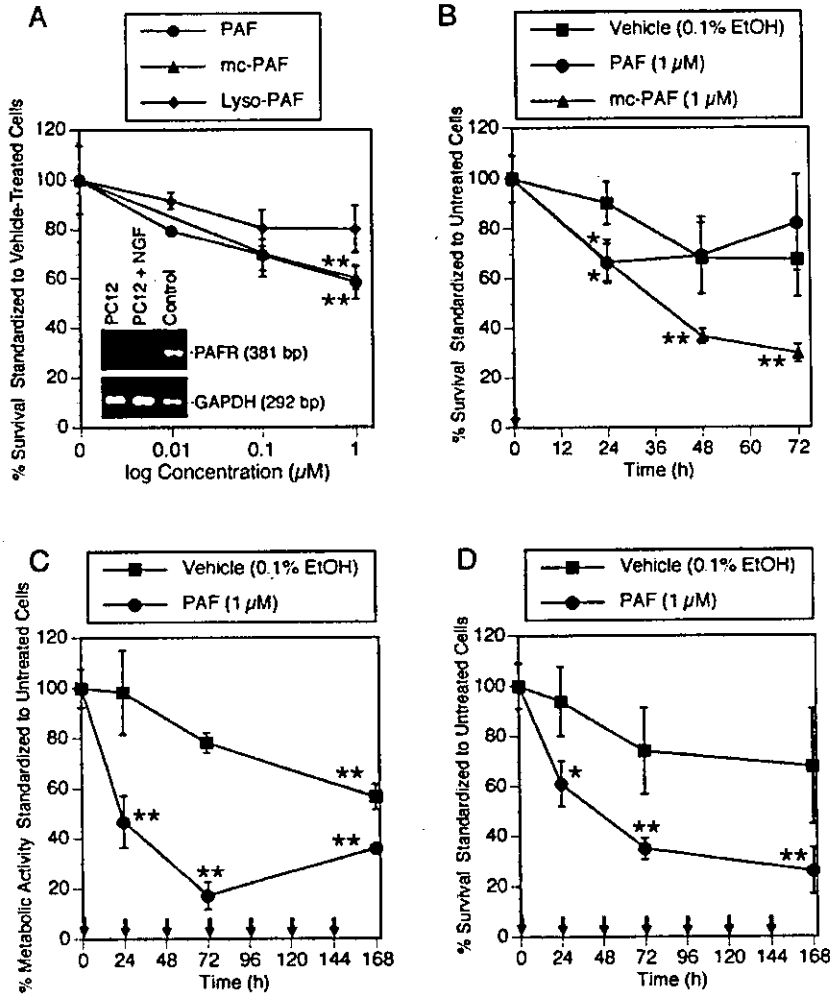

FIG. 1. **The kinetics of PAF-mediated apoptosis initiated independently of PAFR depend upon sustained exposure to active ligand.** *A*, PC12-AC cells were treated for 24 h with PAF (0.01–1 μM), mc-PAF (0.01–1 μM), or *lyso*-PAF (0.01–1 μM) in serum-free treatment media. A dose-dependent decrease in cell number relative vehicle (0.1% EtOH)-treated cells was observed after 24 h of treatment with 1 μM PAF or mc-PAF (**, $p < 0.01$). RT-PCR analysis of PC12-AC cultures (*inset*) confirmed that both PC12-AC cells (*PC12*) and PC12-AC cells differentiated to a neuronal phenotype for 7 days with nerve growth factor (*PC12+NGF*) do not express PAFR mRNA. The positive control was RNA isolated from PC12 cells stably transfected with PAFR. cDNA template integrity was confirmed using GAPDH as an internal standard (*GAPDH*). *B*, PAF (1 μM) treatment resulted in significant cell loss within 24 h of treatment (*, $p < 0.05$) after which no additional reductions in cell number were observed. mc-PAF (1 μM) elicited incremental cell loss for up to 48 h after exposure (*, $p < 0.05$; **, $p < 0.01$). Culture in serum-free treatment media in the presence of vehicle (EtOH, 0.1%) did not affect cell viability until 48 h after treatment. *Arrows* indicate the time of PAF administration. *C*, repeated PAF (1 μM) administration incrementally decreased the metabolic activity of cells for up to 72 h as defined by the ability of mitochondrial dehydrogenases to reduce the formazan salt WST (**, $p < 0.01$). *Arrows* indicate the time when PAF (1 μM) or vehicle (0.1% EtOH) was replenished in fresh media. *D*, incremental cell loss was observed for up to 48 h following chronic PAF (1 μM) treatment. (*, $p < 0.05$; **, $p < 0.01$, ANOVA, post-*hoc* Dunnett's *t* test). As in *C*, media were replaced, and PAF (1 μM) or vehicle (0.1% EtOH) was added every 24 h (*arrows*). *A*, data are expressed as percent survival of vehicle-treated cultures. *B–D*, the data are standardized to untreated cells cultured in treatment media to present the effect of vehicle treatment on cell survival. Results are reported as mean ± S.E. of n = 5–26 cultures per data point.

OpenLab version 3.17. Concentrations of cytosolic B-PAF were estimated in comparison to a B-PAF standard curve resolved in parallel. Data are expressed as pM/PAF-responsive cell following standardization to the number of cells/culture.

Cell Death Assays—PC12-AC cells (8800 cells/cm^2) were plated overnight in complete media in 6-cm diameter tissue culture plates (VWR Scientific). Cells were treated in serum-free RPMI media containing 0.025% BSA (treatment media) for 24–72 h with EtOH (0.1%), PAF (10 nM-1 μM, Biomol Research Laboratories), methyl-carbamyl-PAF (mc-PAF; 100 nM-1 μM, Biomol Research Laboratories), or *lyso*-PAF (10 nM-1 μM, Biomol Research Laboratories). In some cases, cells were pretreated with BN 52021 (1–100 μM, Biomol Research Laboratories), CV-3988 (0.2–2 μM, Biomol Research Laboratories), CV-6209 (1–10 μM, Biomol Research Laboratories), FR 49175 (0.5–50 μM, Biomol Research Laboratories), DFP (0.1 mM or 1 mM, Sigma), DTNB (1 mM, Sigma), or combinations thereof for 15 min followed by addition of PAF (1 μM) for 24 h. Cell survival was assessed by hemocytometer cell counts of trypan blue-excluding cells. Metabolic activity was assessed based on the ability of mitochondrial dehydrogenases, active in viable cells, to reduce the formazan salt, WST-1 (measured at A_{450}–$A_{690\ nm}$, Roche Applied Science). DNA fragmentation was determined by terminal deoxytransferase dUTP nick-end labeling (TUNEL, Roche Applied Science) of cultures fixed for 20 min in 4% paraformaldehyde in 10 mM as described previously (33). Cells, processed for TUNEL, were double-labeled with Hoechst 33258 (0.2 μg/ml) for 20 min at room temperature for additional morphological evidence of apoptotic loss.

RNA Interference Transfection—To suppress expression of the PAF-AH I α_2 subunit, we designed a double-stranded short interfering RNA (siRNA) to the α_2 sequence (AATAAACATGCTTGTCACTCCC/CTGTCTC) and a negative control scrambled sequence (AATGCATAGGAGTTGGAGAGGC/CTGTCTC). Oligonucleotides were obtained from the Biotechnology Research Institute at the University of Ottawa. siRNA duplexes were generated using the Silencer siRNA construction kit (Ambion). Transfection of siRNA was performed with LipofectAMINE 2000 (Invitrogen) and optimized to yield maximal transfection efficiency according to manufacturer's protocol. Briefly, 2 μl of LipofectAMINE 2000 was diluted in 198 μl of RPMI 1640 media for 5 min at room temperature. siRNA duplexes (PAF-AH α_2 or scrambled) were suspended in 100 μl of RPMI 1640 media. PC12-AC cells grown in complete media to 30% confluence in 4-well gelatin-coated Labtek wells were treated with 100 μl of the LipofectAMINE-siRNA complex and incubated for 72 h at 37 °C. Transfection efficiency was determined in

separate cultures by counting EGFP-positive cells upon transfection with pEGFP-C1 as well as morphological changes using β-actin siRNA positive control (Ambion). Because we were unable to obtain >20% transfection efficiency, we co-transfected PAF-AH α_2 or scrambled siRNAs with 0.028 μg/μl of pEGFP-C1 to identify silenced cells. Cells were then exposed to 1 μM PAF in treatment media (RPMI + 0.025% BSA) for either 45 min or 24 h. Data were standardized to the number of EGFP-positive cells in vehicle-treated cultures transfected with pEGFP-C1 only.

Statistical Analysis—Data were analyzed by using ANOVA tests or unpaired Student's *t* tests, as applicable. Following detection of a statistically significant difference in a given series of treatments, *post hoc* Dunnett's *t*-tests or Tukey tests were performed where appropriate. *p* values under 0.05 were considered statistically significant (shown as * or †); *p* values under 0.01 were considered highly statistically significant (shown as ** or ††).

RESULTS

PAF Can Elicit Apoptosis Independently of Its G-protein-coupled Receptor—We have demonstrated previously (11) that PC12-AC cells do not express PAFR but undergo apoptosis-associated DNA fragmentation 24 h after treatment with ≥100 nM PAF and necrotic lysis when treated with >3 μM PAF. In this study, we addressed the kinetics and underlying signaling mechanism of PAF-induced apoptosis in the absence of PAFR (Fig. 1*A*, *inset*). To determine whether cell death is mediated by PAF or downstream PAF metabolites, PC12-AC cells were treated with PAF, mc-PAF, the PAF-AH-resistant synthetic PAF analog (34), or *lyso*-PAF, the immediate PAF metabolite. Both mc-PAF and PAF triggered comparable concentration-dependent cell death 24 h after treatment (Fig. 1*A*). *lyso*-PAF had no significant effect on cell viability (Fig. 1*A*). To establish the kinetics of PAF-mediated cytotoxicity, cell survival was assessed at various times after phospholipid administration. PAF (1 μM) elicited significant cell loss within 24 h of treatment; no further reductions in cell number were detected at 48 or 72 h relative to vehicle controls (Fig. 1*B*). mc-PAF (1 μM) elicited incremental cell loss for up to 72 after treatment (Fig. 1*B*). Comparable kinetics were observed if PAF (1 μM) was replenished in fresh media at 24-h intervals with cells repeatedly treated with PAF exhibiting sustained impairment of cellular metabolic activity (Fig. 1*C*) and an incremental reduction in cell survival (Fig. 1*D*).

To determine whether PAF activates caspases in the absence of PAFR, we examined cleavage of the caspase 3 substrate PARP. Caspase 3-mediated PARP cleavage from 116 to 85 kDa was observed 45 min after a single PAF treatment (Fig. 2*A*). Cleavage markedly increased 3 h after phospholipid administration and was detected for up to 24 h after treatment (Fig. 2*A*) but not at later time points (data not shown). TUNEL-positive cells, evidence of terminal DNA fragmentation, were first observed 24 h after PAF exposure with no evidence of additional death 48 h after exposure (Fig. 2*B*).

Collectively, these findings indicate the following. (*a*) PAF can activate caspase 3 independently of its G-protein-coupled receptor within 45 min of treatment. (*b*) This PAFR-independent apoptotic pathway culminates in terminal DNA fragmentation 24 h after treatment. (*c*) Cell death is not mediated by downstream metabolites. (*d*) Incremental cell death depends upon repeated exposure to active ligand or treatment with PAF-AH-resistant PAF analogs.

Cytosolic PAF-AH Enzymes Limit the Duration of PAF-induced Apoptotic Signaling—These kinetics implicate PAF degradation in the control of apoptotic signaling. To test this hypothesis, we first identified *LIS1*, PAF-AH I α_1, PAH-AH I α_2, and PAF-AH II but not plasma PAF-AH transcripts in PC12 cells by RT-PCR (Fig. 3, *A–F*). Amplicon integrity of the PAF-AH I subunits was verified by sequencing on both strands. We then confirmed protein expression by Western analysis. α_1

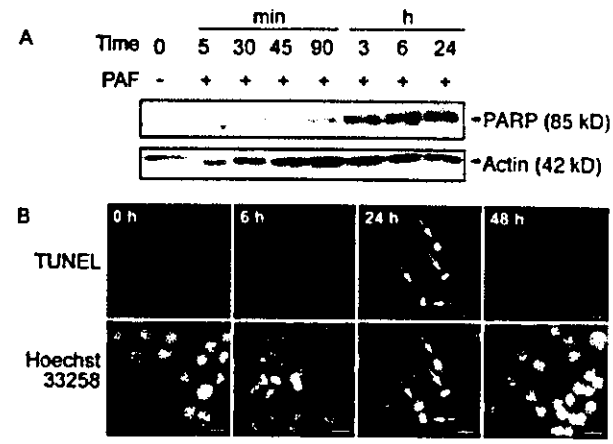

FIG. 2. **PAF triggers a caspase-dependent apoptotic cascade within 45 min of exposure to active ligand.** *A*, PC12-AC cells were exposed to PAF (1 μM) for 24 h and assayed for caspase 3 activity. PARP cleavage to 85 kDa was first detected 45 min after PAF treatment. Blots were re-probed with actin as a loading control. *B*, TUNEL analysis detected apoptosis-associated DNA cleavage (*arrows*, *upper panel*) and DNA condensation (*arrows*, *lower panel*) 24 h after PAF treatment. No additional cell loss was observed 48 h after treatment. *Scale bar*, 10 μm.

protein was constitutively expressed in the presence or absence of PAF (Fig. 3*G*). α_2 protein was present at extremely low levels (Fig. 3, *H* and *I*) with marked induction following exposure to PAF (Fig. 3, *H* and *I*). Closer examination revealed that α_2 protein also increased when cells were cultured in serum-free treatment media suggesting a response to serum withdrawal rather than PAF-specific induction (Fig. 3*I*). LIS1 was constitutively expressed by PC12-AC cells (Fig. 3*J*).

Lacking an antibody to PAF-AH II to verify protein expression, we sequenced the full-length transcript and assayed functional PAF-AH activity in the presence of cytosolic PAF-AH I and II inhibitors. Full-length transcript was amplified from Wistar rat brain and PC12-AC cells using a series of primer pairs homologous to conserved sequences in murine, bovine, and human genes (Table I). A 1173-bp open reading frame was identified in both PC12-AC cells and Wistar rat brain with no base pair mismatches between the sequences.[2] In functional assays, total cytosolic PAF-AII activity in cell lysates was comparable with enzymatic activity in adult mouse brain homogenates (Table II). PAF hydrolytic activity was not detected in treatment media harvested from cells after 24 h of culture confirming the RT-PCR analysis that PC12-AC cells do not express the secreted PAF-AII isoenzyme (Table II). To distinguish between PAF-AH I and PAF-AH II activity, cell lysates were treated with the active serine blocking agent DFP. 0.1 mM DFP inhibits PAF-AII I α_1/α_1 or α_1/α_2 dimer activity, whereas 1 mM DFP inhibits PAF-AH I α_1/α_1, PAF-AH I α_1/α_2, and PAF-AH II activity. PAF-AH I α_2/α_2 dimers are DFP-resistant (21, 23, 35). 68–70% of the total cytosolic PAF-AH activity was blocked by 0.1 mM DFP indicative of PAFAH I α_1/α_1 or α_1/α_2 activity (Table II). Increasing the DFP concentration to 1 mM blocked an additional 4–7% of PAF-AH activity attributed to PAF-AH II. DFP-resistant PAF-AH I α_2/α_2 homodimer activity composed 25% of cytosolic PAF-AH activity in lysates extracted from cells cultured in complete media.

The kinetics of PAF hydrolysis by PAF-AH I and II were established using the fluorescent PAF substrate B-PAF. Cells were treated with 1 μM B-PAF to initiate apoptotic signaling. B-PAF and its metabolites were extracted at various time points using a modified Bligh and Dyer procedure and identi-

[2] The rat PAF-AH II cDNA cloned from adult Wistar rat brain was deposited under GenBank™ accession number AY225592.

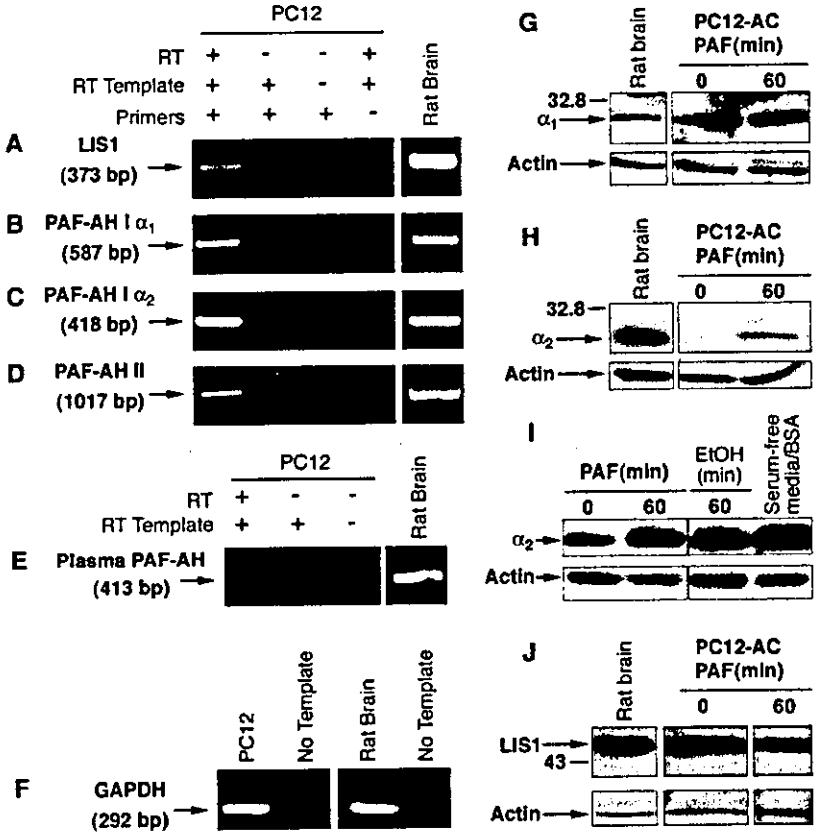

FIG. 3. **Expression patterns of PAF-AH I, PAF-AH II, and plasma PAF-AH in PC12-AC cells.** RT-PCR was performed for LIS1 (*A*), PAF-AH I α_1 (*B*), PAF-AH I α_2 (*C*), and PAF-AH II (*D*). Plasma PAF-AH mRNA was not detected (*E*). The absence of genomic DNA contamination or reagent contamination was confirmed by the control reactions: no RT during the RT reaction, no template during the PCR reaction, and no primers during the PCR reaction. Rat brain RNA was reverse-transcribed as a same-species positive control (*Rat Brain lane*). Template integrity of the random-primed PC12-AC RT product was verified by using GAPDH (*F*). Equal amounts of protein (30 μg) from cells cultured in complete media (*0*) or cells treated for 60 min with 1 μM PAF in treatment media (*60*) were separated under reducing conditions and immunoblotted for α_1 (*G*), α_2 (*H* and *I*), or LIS1 (*J*). Protein lysates from neonatal rat brain were used as a same-species positive control. Representative immunoblots of replicate experiments are depicted. PAF-AH α_1 was constitutively expressed (*G*). Significant PAF-AH α_2 protein was not detected until cells were treated with PAF (1 μM) (*H*). Longer exposure times (overnight) indicated that PC12-AC cells expressed low levels of protein and that serum deprivation was sufficient to induce α_2 protein expression (*I*). LIS1 was constitutively expressed (*J*). Blots were probed for actin as a loading control (*G–J*).

TABLE I
Primer pairs used to detect cytosolic and plasma PAF-AH transcript by RT-PCR

Gene	Strand	Sequence (5′–3′)	Amplicon size
			bp
GAPDH	Sense	TGGTGCTGAGTATGTCGTGGAGT	292
	Antisense	AGTCTTCTGAGTGGCAGTGATGG	
PAF-AH I α_1	Sense	GACGGACGCTGGATGTCTCT	587
	Antisense	AGACGAAGCAGCAAGGAGTG	
PAF-AH I α_2	Sense	TGCAGCAGTACGAGATATGG	418
	Antisense	AACATGTCGTGGCAGGAGAT	
PAF-AH I LIS1	Sense	CTGCTTCAGAGGATGCTACA	373
	Antisense	ATCAGAGTGCCGTCCTGATT	
PAF-AH II1	Sense	GGATGTGATGGAGGGTC	1017
	Antisense	TGCTTCTGCAGGAAGGCCAA	
PAF-AH II2	Sense	CAGCTGGTGATGAGATGG	224
	Antisense	GCGCTTGTTATACTGCAGGT	
PAF-AH II3	Sense	TGAGCCGAGTGGCTGTGATG	472
	Antisense	CCCTTGGATGAGCGATGGTC	
PAF-AH II4	Sense	CAGCTGGTGATGAGATGG	1250
	Antisense	CAACCTAGAGGCTGGACAGA	
Plasma PAF-AH	Sense	GGGGCATTCTTTTGGAGGAG	413
	Antisense	GACAGTCCCACTGATCAAAGTC	
PAFR	Sense	CACTTATAACCGCTACCAGGCAG	381
	Antisense	AAGACAGTGCAGACCATCCACAG	

fied by TLC. Fluorescent intensity was quantified by comparison to resolved fluorescent standards. Cytosolic and extracellular lipids were fractionated from B-PAF-treated cultures with an acidified methanol wash separating phospholipids bound to proteins on plasma membrane from internalized lipids (36). We found that 1 μM B-PAF was stable in cell-free, serum-free treatment media at 37 °C for at least 60 min; no degradation to B-*lyso*-PAF was observed in the absence of cells (Fig. 4*A*). B-PAF was rapidly internalized by PC12-AC cells (Fig. 4*B*, *extracellular*) with concentrations reaching ~16–20

TABLE II
PAF-AH activity in PC12-AC cells, mouse brain lysate, and tissue culture media

PAF-AH activity[a]							
	PC12-AC lysates				Cell-free media		
Mouse brain lysate, positive control	Untreated lysates	% inhibition[b]					
		Time	0.1 mM DFP	1 mM DFP	Complete media	Serum-free treatment media	PC12-AC-conditioned treatment media
	nmol/min/μg or % inhibition	*min*	*nmol/min/μg or % inhibition*			*nmol/min/μg or % inhibition*	
1.97 ± 0.44 n = 8	1.37 ± 0.19 n = 23	15	68% n = 6	75% n = 5	3.36 ± 0.10 n = 2	0.01 ± 0.00 n = 2	0.00 ± 0.00 n = 3
		30	70% n = 3	74% n = 3			

[a] Data represent mean ± S.E. n denotes the number of replicates conducted over 1–4 experiments.
[b] Lysates were pretreated for 15 or 30 min at room temperature with vehicle (10 mM PBS) or the indicated concentrations of DFP. Activity in vehicle-treated cultures was equivalent to that detected in untreated cultures. % inhibition was determined as described under "Materials and Methods."

pM/cell within 5 min of incubation (Fig. 4*B*, *cytosolic*). Internalized B-PAF levels remained constant for 60 min dropping to 6–8 pM/cell by 75 min (Fig. 4*B*, *cytosolic*). B-PAF degradation was detected within 15 min of internalization (Fig. 4*C*, *vehicle*). A linear rate of metabolism (r^2 = 0.97) was observed for up to 75 min (Fig. 4*C*, *vehicle*). Closer examination of the fate of B-PAF metabolite by fractionation revealed that B-*lyso*-PAF was released from cells in two stages (Fig. 4*D*). Between 5 and 15 min of incubation, 50% of internalized B-PAF was converted to B-*lyso*-PAF (Fig. 4*D*, *Cytosolic*) and secreted from the cells (Fig. 4*D*, *extracellular*). Between 30 and 60 min, B-*lyso*-PAF was not released and accumulated in the cell cytosol (Fig. 4*D*, *cytosolic*). A delayed phase of secretion was observed between 60 and 75 min (Fig. 4*D*, *extracellular*).

To track the fate of secreted B-*lyso*-PAF, we performed quantitative time-lapse fluorescence microscopy (Fig. 4*E*). B-PAF-containing media were removed, and cells were washed with PBS containing 1% BSA at various time points to remove free lipids loosely associated with the plasma membrane but not phospholipids bound to membrane proteins. Cells were photographed, and the B-PAF-containing media were replaced. A linear increase in cell-associated fluorescence was observed over the first 70 min of exposure (r^2 = 0.97) followed by a plateau in cell-associated B-PAF (Fig. 4*E*).

Taken together, these data indicate that PAF administered to cells is metabolized by PAF-AH I and II with a $t_{1/2}$ of 75 min (where $t_{1/2}$ is the time to reach half-maximal concentrations). The PAF metabolite, *lyso*-PAF, is secreted from cells but remains bound, apparently to carrier proteins, on the extracellular surface of the plasma membrane.

Cytosolic PAF-AHs Can Be Targeted Pharmacologically to Promote Cell Survival—The kinetics of PAF-induced apoptosis (Figs. 1 and 2) and PAF degradation (Fig. 4) suggest that cytosolic PAF concentrations must remain elevated for at least 60 min to elicit apoptosis. This hypothesis predicts that compounds capable of inhibiting PAF internalization or increasing cytosolic PAF-AH activity will block PAF-mediated death triggered independently of PAFR. To test this hypothesis, we evaluated the anti-apoptotic actions of four PAF antagonists (CV-3988, CV-6209, BN 52021, and FR 49175). These compounds were chosen because of their affinities for different PAF-binding sites identified pharmacologically. CV-3988 and CV-6209 are competitive PAF antagonists that preferentially interact with synaptosomal and microsomal PAF-binding sites (17). CV-3988 competes for PAF at the plasma membrane, likely PAFR, as well as interacting with intracellular microsomal binding sites, likely internalized PAFR (17). CV-6209 preferentially interacts with a single binding site in microsomal membranes (17). BN 52021 (also known as ginkgolide B) is a noncompetitive PAF antagonist with affinity for three discrete PAF-binding sites (17) as well as potent antioxidant activity (37). FR 49175 is a fungal metabolite derivative that inhibits PAF-induced biological activity through unknown mechanisms (38, 39). Treatment of PC12-AC cells with CV-3988, BN 52021, or FR 49175 had no effect on cell survival (Fig. 5, *A–C*); however, CV-6209 was toxic to cells at concentrations above 1 μM (Fig. 5*D*). We observed significant concentration-dependent anti-apoptotic activity when cells were preincubated for 15 min with BN 52021 (1–100 μM) or FR 49175 (0.5–50 μM) and then exposed to PAF (Fig. 5*E*). Both BN 52021 and FR 49175 inhibited PAF-mediated caspase 3 activation as assessed by PARP cleavage (Fig. 5*F*). CV-3988 (0.1–10 μM) and CV-6209 (0.01–1 μM) did not exhibit anti-apoptotic activity (Fig. 5*E*).

We next tracked B-PAF fate by lipid extraction and TLC in the presence or absence of BN 52021 and FR 49175 to establish whether these antagonists affect phospholipid internalization or PAF-AH activity. FR 49175 and BN 52021 did not alter the rate or extent of B-PAF internalization (Fig. 6, *A* and *D*, *extracellular*). In both antagonist- and vehicle-treated cultures, maximal cytosolic B-PAF levels were attained within 5 min of B-PAF exposure (Fig. 6, *A* and *D*, *cytosolic 5 min*). We did not observe an increase in total B-PAF hydrolysis. Cytosolic B-PAF concentrations, estimated at 8 pM/cell, in BN 52021- and FR 49175-treated cultures were comparable with vehicle-treated cells by the end of the 75 min test period (Fig. 6, *A* and *D*, *cytosolic, 75 min*). Significantly, we found that FR 49175 and BN 52021 accelerated both the kinetics of B-PAF degradation (Fig. 6, *A* and *D*, *45 min*) and the release of B-*lyso*-PAF into the media (compare Fig. 6, *B* and *E*, *cytosolic 45 min* and *C* and *F*, *extracellular, 45 min*). By 45 min, 39 (FR 49175) or 41% (BN 52021) of exogenous B-PAF had been converted to B-*lyso*-PAF compared with 29% in vehicle-treated cells. This acceleration dropped cytosolic B-PAF levels more rapidly in antagonist-treated cultures from 16 pM/cell (5 min) to 10 pM/cell (45 min) in the presence of FR 49175 or 8 pM/cell (45 min) in the presence of BN 52021 (Fig. 6, *B* and *E*). Maximal release of B-*lyso*-PAF from cells was observed within 45 min in antagonist-treated cultures compared with 75 min in vehicle-treated cultures (Fig. 6, *C* and *F*). 50% of the released metabolite diffused or was transported back into the cells within 75 min in FR 49175 treated cultures; 32% of B-*lyso*-PAF re-entered cells in BN 52021-treated cultures (Fig. 6, *B–F*).

PAF-AH I α_2/α_2 Activity Is Anti-apoptotic—To determine how BN 52021 and FR 49175 accelerate PAF-AH hydrolysis, we examined PAF-AH I α_1 and α_2 expression. Cells were preincubated in serum-free treatment media with vehicle (Me_2SO), BN 52021, or FR 49175 for 15 min before addition of PAF (Fig. 7). We found PAF-AH α_1 expression remained constant whether cells were cultured in complete media, serum-free treatment media, pretreated with Me_2SO, or exposed to PAF (Fig. 7*A*,

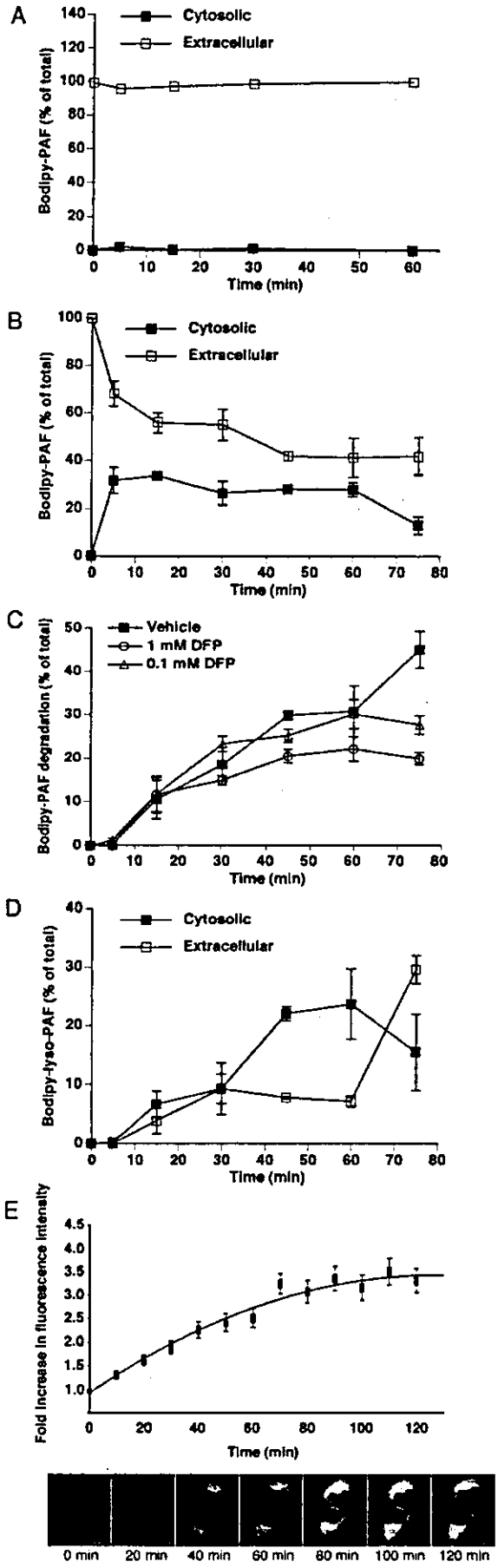

FIG. 4. **Internalization, kinetic analysis, and metabolic fate of B-PAF and B-*lyso*-PAF in PC12-AC cells.** PC12 cells were incubated with 1 μM B-PAF at 37 °C for 0, 5, 15, 30, 45, 60, and 75 min. At each time point, lipids were extracted from the extracellular and cytosolic fractions and were separated by TLC. *A–C*, data represent relative fluorescence of B-PAF in each fraction expressed as a percentage of the total fluorescent lipids recovered. Data are the mean of 2–4 independent experiments conducted in replicate. *A*, B-PAF was not degraded by treatment media in the absence of PC12 cells. *B*, in cell cultures, B-PAF was rapidly internalized within 5 min (*extracellular fraction*) after which levels remained stable until 60 min and dropped by 75 min (*cytosolic fraction*). *C*, conversion of B-PAF to B-*lyso*-PAF was monitored to determine the degree of PAF hydrolysis in the presence or absence of the PAF-AH I α_1 and PAF-AH II inhibitor DFP. Cells were pretreated for 15 min in treatment media with vehicle (PBS) or DFP before addition of B-PAF. *D*, the fate of the B-PAF metabolite B-*lyso*-PAF was followed by fractionation. *E*, to determine whether B-*lyso*-PAF secreted from cells remains loosely associated with the lipid bilayer or bound to membrane proteins, cell-associated fluorescence was tracked by live-cell imaging. The B-PAF containing media were removed every 10 min, and cells were washed with PBS + 1% BSA to remove phospholipids at the extracellular face of the plasma membrane but not lipids associated with membrane proteins. Data are reported as the mean increase in fluorescence intensity standardized to background fluorescence in untreated cells ± S.E. (n = 16–25 per data point). Cell-associated fluorescence increased 3-fold over the first 75 min of exposure and remained constant between 75 and 120 min despite repeated washes indicating that the secreted material removed by the acidified methanol wash (*D*, *extracellular*) was likely bound to proteins at the plasma membrane (*E*). *Scale bars*, 5 μm.

PAF). Surprisingly, PAF-AH α_1 protein levels decreased progressively over the first 30 min of PAF treatment and remained low until the end of the 90-min test period (Fig. 7*A*, *BN 52021*). Comparable results were observed in FR 49175-treated cultures (Fig. 7*A*, *FR 49175*). α_2 expression was not altered by BN 52021 or FR 49175 in that protein expression increased dramatically during the 15-min preincubation period in serum-free treatment media regardless of antagonist or vehicle administration and remained elevated over the 90 min PAF test period (Fig. 7*B*).

The finding that both compounds accelerate PAF degradation by reducing PAF-AH I α_1 subunit expression was unexpected. Two alternative, but not mutually exclusive, explanations lie in the possibility that this reduction in α_1 expression promotes formation of PAF-AH I α_2/α_2 homodimers and/or that PAF-AH II activity is increased. Following exposure to PAF in serum-free media, the catalytic composition of PAF-AH I would be expected to change from a predominance of α_1/α_1 homodimers in control cultures (Table I) to α_1/α_2 heterodimers and α_2/α_2 homodimers given the 8–10-fold increase in α_2 protein expression (Figs. 3 and 7). In cultures pretreated with BN 52021 or FR 49175, suppression of α_1 protein expression likely favors a more a rapid transition from α_1/α_1 to α_2/α_2 homodimers following PAF exposure. This hypothesis is supported by the dramatic increase in the α_2 to α_1 ratio observed 30–90 min after PAF exposure in BN 52021 and FR 49175-treated cultures relative to vehicle (Fig. 7*C*). Alternatively, in addition to effects on PAF-AH α_1, BN 52021 and/or FR 49175 may alter PAF-AH II activity, an enzyme with proven anti-apoptotic properties (26).

To address these possibilities, we performed three loss of function studies. First, we treated cells with 0.1 mM DFP to inhibit PAF-AH I α_1/α_1 and α_1/α_2 catalytic activity without changing the relative ratio of α_1 to α_2 protein expression (21, 23, 35). In the unlikely event that the anti-apoptotic effects of BN 52021 and FR 49175 are mediated by a loss of α_1 catalytic activity, then 0.1 mM DFP should be cytoprotective. Cells were exposed for 15 min (Fig. 4*C* and Fig. 8*A*) before addition of B-PAF. DFP did not affect B-PAF internalization (data not shown) but reduced B-PAF degradation by 38% 75 min after B-PAF exposure (Fig. 4*C*, *0.1 mM DFP, 75 min*). To ensure intracellular concentrations of DFP reached 0.1 mM by the time cells were exposed to PAF, we extended the preincubation

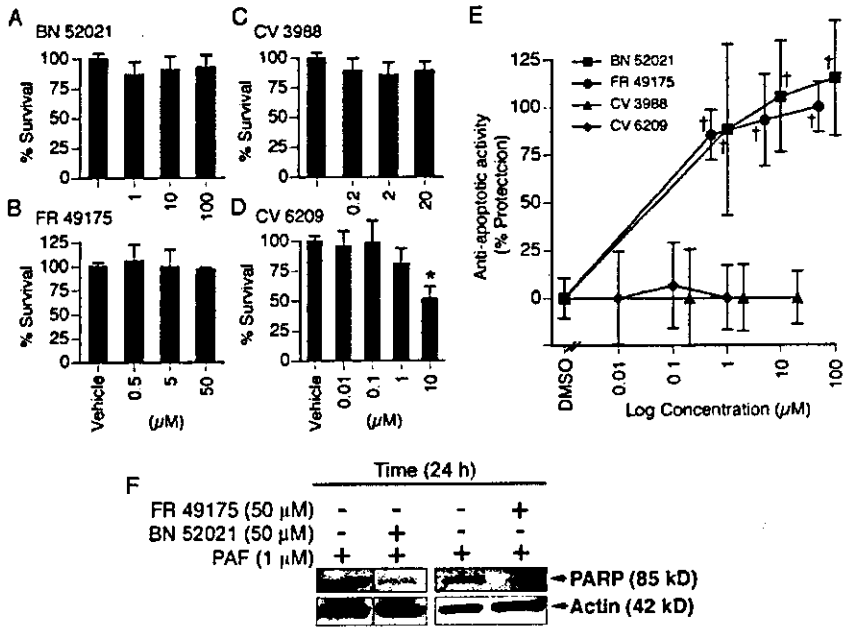

FIG. 5. **Anti-apoptotic actions of the PAF antagonists BN 52021 and FR 49175 but not CV-6209 or CV-3988 in PAFR-negative cells.** PC12-AC cells were pretreated for 15 min with 0.1% Me_2SO (*DMSO, vehicle*) or different concentrations of PAF antagonists and exposed to 0.1% EtOH (*A–D*) or PAF 1 μM (*E* and *F*) for 24 h. *A–E*, data are expressed as percent survival of vehicle-treated cultures. Results are reported as mean ± S.E. of $n = 5–47$ cultures per data point. BN 52021, FR 49175, and CV-3988 had no effect on the viability of vehicle-treated cultures. CV-6209 (10 μM) was toxic (*, $p < 0.05$). BN 52021 and FR 49175 but not CV-3988 or CV-6209 dose-dependently inhibited PAF-mediated death (†, $p < 0.05$; ††, $p < 0.01$). *F*, BN 52021 and FR 49175 inhibited PAF-mediated caspase 3 activation as assessed by PARP cleavage.

period from 15 to 30 min with no additional effects on the kinetics of PAF-AH inhibition (data not shown). Inhibition of PAF-AH I α_1/α_1 and α_1/α_2 catalytic activity did not alter survival of cells treated for 24 h with vehicle (Fig. 8*A*, *vehicle (0.1% EtOH)*) and did not intensify PAF-mediated cell death (Fig. 8*A*, *PAF*). These data suggest that PAF-AH I α_1 does not play a significant role in regulating PAF-induced apoptosis.

Second, to determine the role of PAF-AH II in control of PAF-mediated cell death, we treated cultures with PAF (1 μM) or PAF vehicle (0.1% EtOH) in the presence of DFP, the sulfhydryl blocking reagent (DTNB), or vehicle (PBS) (Figs. 4*C* and 8*A*). Cells were pre-exposed to 1 mM DFP or 1 mM DTNB for 15 (Figs. 4*C* and 8*A*) or 30 min (data not shown) before treatment with PAF or vehicle. Individually, DFP and DTNB were found to have no effect on the survival of vehicle-treated cells (Fig. 8*A*, *vehicle (0.1% EtOH)*). Increasing the DFP concentration from 0.1 to 1 mM inhibited 55% of B-PAF degradation within 75 min indicating that 17% of DFP-sensitive PAF-AH activity was PAF-AH II (Fig. 4*C*, *1 mM DFP, 75 min*). Despite this substantial inhibition of PAF hydrolysis (55%), PAF-mediated cell loss was intensified by only 8% (Fig. 8*A*, *1 mM DFP*). To confirm these results, we used a pharmacological agent that, unlike DFP, inhibits PAF-AH II but not PAF-AH I through different mechanisms. Exposure to 1 mM DTNB elicited the same results as 1 mM DFP (Fig. 8*A*, *DTNB*). To ensure complete inhibition of PAF-AH II, we exposed cells to both DFP and DTNB. Combination treatment reportedly abolishes activity of purified PAF-AH II (35). Preincubation in DFP and DTNB followed by 24 h of exposure to EtOH decreased vehicle-treated cell survival by 12% (Fig. 8*A*, *vehicle (0.1% EtOH)*). Combination of treatments reduced PAF-treated cell survival by 20%, likely the cumulative results of inhibitor toxicity (12%) and PAF-AH II inhibition (8%) (Fig. 8*A*, *PAF*). These findings suggest that (*a*) PAF-AH I α_1 activity is not anti-apoptotic and (*b*) that although PAF-AH II activity is cytoprotective, PAF-AH II plays a secondary role to PAF-AH I α_2 in regulating PAF-mediated apoptosis.

The data point to PAF-AH I α_2 as a potential therapeutic target to reduce apoptogenic PAF concentrations under diverse pathophysiological conditions. To confirm this role directly, we acutely suppressed α_2 expression using an RNAi strategy. PAF-AH I α_2-specific RNAi but not the scrambled control or transfection reagent alone reduced α_2 protein expression (Fig. 8*B*). Because we were unable to achieve >20% transfection efficiency, we could not knockdown PAF-AH I α_2 expression in all cells. To identify transfected cells, we co-transfected cultures with EGFP in combination with α_2-specific or scrambled siRNAs (Fig. 8*C*). To control for possible cytotoxic effects of siRNAs, parallel experiments were performed in which cultures were transfected with EGFP alone, and survival was expressed relative to EGFP-positive vehicle-treated cells. Most importantly, PAF-AH I α_2 RNAi down-regulation significantly enhanced PAF-mediated cytotoxicity (Fig. 8*C*).

DISCUSSION

PAF-like lipids have been implicated as key apoptotic second messengers induced by a variety of pathological stressors (6, 19, 20, 25, 26, 29, 30, 33, 40). Converging evidence points to PAFR activation of the conserved mitochondrial death pathway (6, 12, 18–20, 41). Our previous work has demonstrated that PAF can also transduce cell death independently of its G-protein-coupled receptor (11), but it is not known how cell death is regulated in the absence of PAFR. The importance of this apoptotic cascade is underlined by the fact that neurons express low levels to no PAFR (33, 42), and yet PAF is a principal mediator of neuronal loss in ischemia, encephalitis, epileptic seizure, meningitis, and human immunodeficiency virus-1 dementia (1–5). To provide mechanistic insight into this PAFR-independent pathway, we show the following. 1) PAF can initiate caspase-dependent cell death in the absence of it G-protein-coupled receptor. 2) The duration of PAF apoptogenic signaling is regulated by the α_2 subunit of PAF-AH I and, to a lesser extent, by PAF-AH II. 3) PAFR-independent cell death can be inhibited by two PAF antagonists: the gingkolide BN 52021 and the fungal derivative FR 49175 but not by CV-3988 or CV-6209. 4) Both BN 52021 and FR 49175 protect cells from PAF-induced cell death by reducing PAF-AH I α_1 protein levels indirectly promoting PAF-AH I α_2 homodimer activity.

Apoptotic PAF Signal Transduction in the Absence of PAFR—To provide mechanistic insight into how PAF transduces cell death in the absence of PAFR, we followed the internalization and metabolic fate of Bodipy fluorophore-conjugated PAF in PAF-sensitive cells (11, 43). PC12 cells express all of the components of both cytosolic PAF-AH enzymes (I and

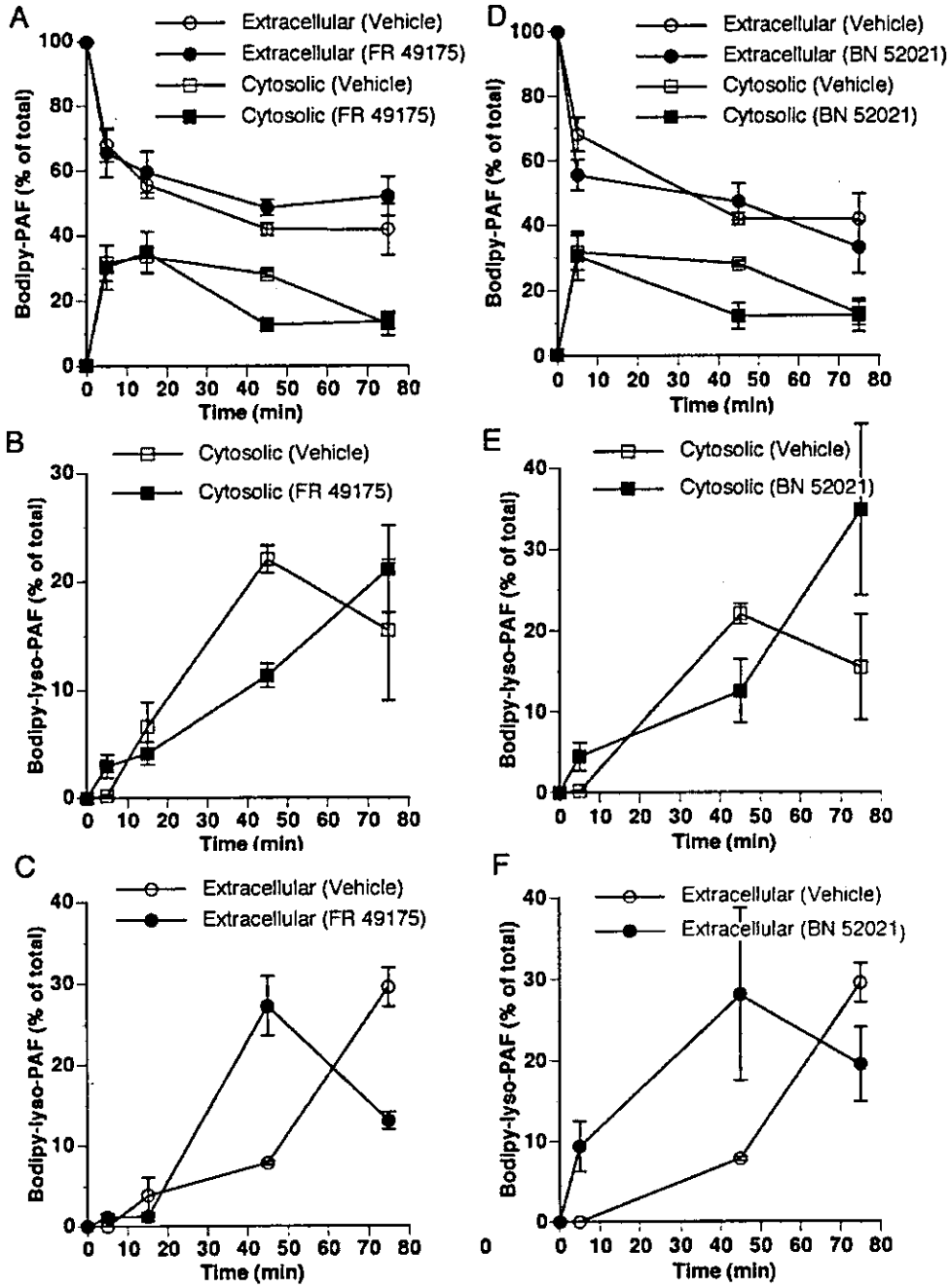

FIG. 6. **FR 49175 and BN 52021 accelerate the kinetics of PAF-AH activity.** PC12-AC cells were pretreated with FR 49175 (10 μM), BN 52021 (50 μM), or PBS (vehicle) for 15 min and then incubated with 1 μM B-PAF at 37 °C. Lipids were extracted from the extracellular and cytosolic fractions and separated by TLC. The relative fluorescence of B-PAF or B-*lyso*-PAF in each fraction is expressed as the percentage of the total fluorescent lipids recovered. Data represent the mean ± S.E. of n = 4 (FR 49175) or n = 8 (BN 52021) independent experiments conducted in replicate. *A*, FR 49175; *D*, BN 52021 had no effect on B-PAF internalization (*extracellular*), but cytosolic B-PAF levels were reduced within 45 min of exposure (*cytosolic*). *B* and *E*, the kinetics of B-PAF degradation and (*C* and *F*) release were accelerated in FR 49175- (*B* and *C*) and BN 52021 (*E* and *F*)-treated cells.

II) but not plasma PAF-AH or PAFR. Extracellular PAF was internalized by PC12 cells with a $t_{1/2}$ of ~5 min. Downstream activation of caspase 3 was initiated when cytosolic PAF concentrations were elevated by ~15–20 pM/cell. These findings complement previous work demonstrating that exposure to oxidative stressors triggers apoptogenic remodeling of membrane phospholipids into PAF-like lipids (26) and provide strong evidence that cytosolic accumulation of PAF and PAF-like lipids can trigger apoptotic death independently of PAFR. In fact, internalization of PAF mediated by PAFR endocytosis (36) may protect cells from this cell death cascade. Endocytosis of the PAF·PAFR complex triggers release of plasma PAF-AH from macrophages thereby reducing extracellular ligand concentrations (36).

Although we have yet to identify the effector proteins responsible for transducing increases in intracellular PAF concentration into downstream caspase activation, our data indicate that the temporal kinetics of PAF accumulation regulate the duration of apoptotic signaling and that PAFR-independent cell death is triggered by PAF and not by its immediate metabolite *lyso*-PAF. We found that intracellular PAF levels must remain elevated by approximately 60 min to elicit significant apoptotic death. Decreasing cytosolic concentrations to less than 10 pM/cell of exogenous PAF stops the cell death signaling. *lyso*-PAF,

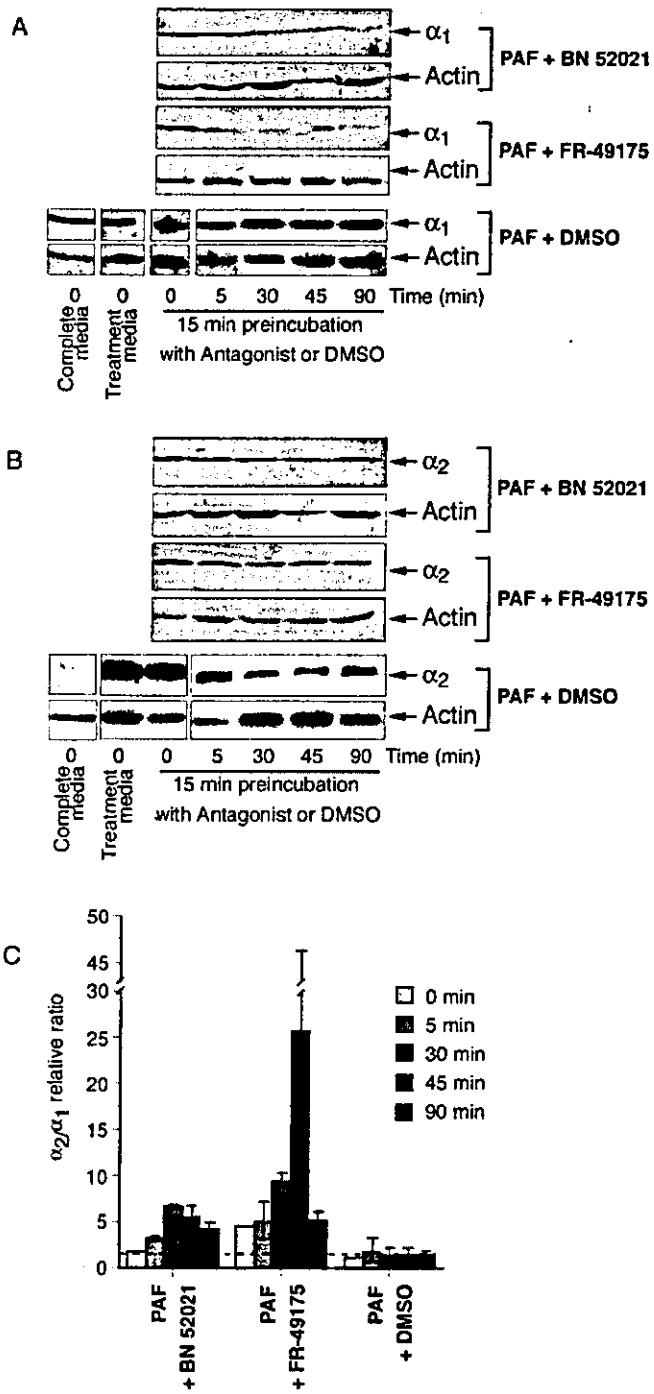

FIG. 7. **BN 52021 and FR 49175 increase the relative ratio of PAF-AH I α_2 to α_1 expression following PAF challenge.** PC12 cells were treated with PAF (1 μM) following a 15-min preincubation in the presence or absence of BN 52021 (50 μM), FR 49175 (50 μM), or vehicle (0.1% Me_2SO (*DMSO*)). Immunoblotting was performed for α_1 (*A*) or α_2 (*B*). BN 52021 and FR 49175 reduced α_1 expression (*A*) without affecting the α_2 induction (*B*). Blots were reprobed for actin as a loading controls (*A* and *B*). α_1 (*A*) and α_2 (*B*) protein levels were standardized to actin and expressed as a percent of the basal expression in cells cultured in complete media. *C*, the relative ratio of α_2 to α_1 protein following BN 52021 or FR 49175 revealed a stoichiometric increase in the levels of α_2 compared with α_1 relative to cells exposed to PAF in the absence of antagonist.

the immediate PAF metabolite, does not transduce downstream apoptotic induction given that equimolar concentrations of *lyso*-PAF are not cytotoxic and that the endogenous metabolite remains cell-associated without detectable effect. Accelerating the kinetics of PAF degradation with BN 52021 or FR 49175 reduces PAF concentration to sub-apoptotic levels (approximately >8 pM/cell) within 45 min and prevents PAF-induced caspase activation. The PAFR-specific antagonists CV-3988 and CV-6209 have no effect on PAF-mediated PAFR-independent cell death when administered at concentrations up to 20 times that of their reported IC_{50} antagonist activities (44–46). Most interestingly, the anti-cell death activities of the antagonists tested in this study (FR 49175 > BN 52021 > CV-3988 or CV-6209) are in direct opposition to their PAF antagonist potency in other biological assays (CV-6209 > CV-3988 > BN 52021 > FR 49175) (38, 44–47), suggesting that their PAFR-independent anti-apoptotic actions are inversely proportional to their affinity for PAFR.

We do not know how PAF is internalized by PC12 cells in the absence of its G-protein-coupled receptor. In addition to endocytosis as a PAF·PAFR complex, active trafficking of PAF across the plasma membrane is accomplished by a PAF-specific transglutaminase and by interaction with low affinity binding sites yet to be identified at the molecular level (14, 48). Passive PAF internalization is regulated by transbilayer movement (flipping) across the plasma membrane occurring as a result of physicochemical changes in membrane properties accompanying cellular activation (15). It has been suggested that PAF internalization in the absence of PAFR is not rapid enough to elicit acute biological activity in hematopoietic cells (36, 49). In this study, we present evidence that PAFR-independent PAF internalization by nonhematopoietic cells is indeed sufficient to trigger apoptotic cell loss.

PAF-AH α_2 Activity Is Anti-apoptotic—Administration of recombinant PAF-AH II or plasma PAF-AH and ectopic overexpression protects cells from death elicited by low density lipoprotein, glutamate, or oxidative stress (25, 26, 29–31). In this study, we show that PAF-AH I exerts similar cytoprotective effects with three important distinctions. First, the anti-apoptotic actions of PAF-AH I are subunit-specific. Under normal culture conditions, we found PAF hydrolysis in PC12 cells to be primarily mediated by the PAF-AH I α_1 subunit and to a lesser extent by PAF-AH II. Following serum deprivation and exposure to pathological PAF concentrations, PAF-AH I α_2 but not PAF-AH I α_1, protein expression is acutely up-regulated. By pharmacological inhibition using DFP and DTNB and by RNA interference, we found that PAF-AH I α_2 but not PAF-AH I α_1 activity reduces the duration of PAF-mediated apoptotic signaling. When cells were cultured under normal conditions, we found that cytosolic PAF-AH activity is PAF-AH 1 α_1/α_1 and α_1/α_2 (~70%) > PAF-AH I α_2/α_2 (~25%) > PAF-AH II (5%). When cells were deprived of serum and challenged with PAF, this activity profile shifted in favor of PAF-AH I α_2/α_2 (45%) > PAF-AH α_1/α_1 or α_1/α_2 (38%) > PAF-AH II (17%). Most surprisingly, pharmacological inhibition of α_1 enzymatic activity had no effect on PAF-mediated cell death, whereas suppression of α_2 induction by RNA interference significantly enhanced cell loss providing strong evidence for anti-apoptotic subunit specificity.

Second, PAF-AH I α_2 is mobilized as part of an endogenous cell survival response. These findings complement studies documenting the anti-apoptotic actions of plasma PAF-AH and PAF-AH II (8, 25, 26, 29–31). Moreover, we find that PAF-AH II is not able to compensate for a loss of PAF-AH I α_2 function. In fact, we were surprised to find that a 55% reduction in PAF hydrolysis observed 75 min after PAF challenge following DFP treatment only moderately enhanced PAF-mediated cell death. The kinetics of PAF-AH activation may explain the lack of significant PAF-AH II protection. PAF-AH α_2 is mobilized acutely in response to serum withdrawal, but an increase in DFP- or DTNB-sensitive PAF-AH II activity is only observed

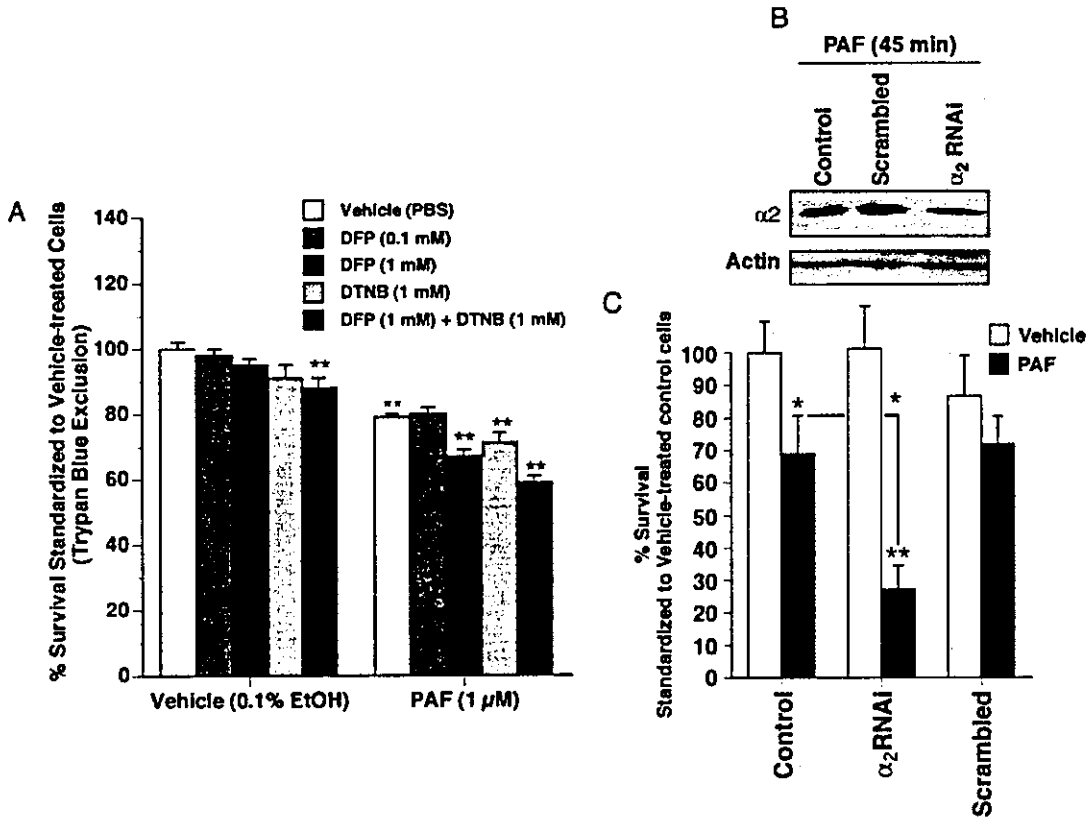

FIG. 8. **PAF-AH α_2 activity is anti-apoptotic.** *A*, PC12 cells were treated with PAF (1 μM) or ethanol (0.1%) at 37 °C for 24 h following 15 min of preincubation with DFP (0.1 mM), DFP (1 mM), DTNB (1 mM), or DFP (1 mM) + DTNB (1 mM) to abolish PAF-AH α_1 and PAF-AH II activity. Cell survival was assessed as described in Fig. 5. Inhibition of PAF-AH II but not PAF-AH α_1 activity moderately intensified PAF-mediated death. (ANOVA, *post hoc* Tukey tests, *, $p < 0.05$; **, $p < 0.01$). *B*, short interfering RNA oligonucleotides were employed to silence PAF-AH α_2. Western analysis for α_2 was performed at various time points after transfection following a 45-min treatment with PAF (1 μM) in serum-free treatment media. A partial knockdown in α_2 protein levels, consistent with the maximal 20% transfection efficiency, was detected 72 h after transfection (α_2 *RNAi*) compared with nontransfected cells (*control*) or cells that had been transfected with nonspecific scrambled RNAi (*scrambled*). β-Actin blot was performed as a loading control. *C*, PC12 cells were transfected with pEGFP-C1 (*control*) or co-transfected with pEGFP-C1 and α_2 RNAi (α_2 *RNAi*) or scrambled RNAi (*scrambled*). 72 h after transfection, cells were treated with PAF (1 μM) or vehicle (0.1% EtOH) for 24 h. Data are expressed as % survival of EGFP-positive cells standardized to vehicle-treated controls. Survival was reduced to 28% in cells transfected with α_2 RNAi compared to 70% in EGFP-transfected cells. *Asterisks* indicate statistically significant differences by Student's *t* test.

after 30–60 min of PAF exposure. Only PAF-AH I α_2 was found to reduce apoptogenic concentrations of cytosolic PAF within the first 30 min of exposure. PAF-AH II is mobilized as part of a delayed cell survival program possibly to ensure that "sub-apoptotic" PAF concentrations are maintained.

Third, and perhaps most importantly, the anti-apoptotic response afforded by shifting the PAF-AH I α_1 subunit expression in favor of α_2 can be enhanced by PAF antagonists. Pharmacological suppression of α_1 by BN 52021 or FR 49175 accelerates the kinetics of PAF deacetylation to *lyso*-PAF and protects cells from PAF-mediated apoptosis. Although it would at first appear counterintuitive that a reduction in PAF-AH subunit expression enhances PAF hydrolysis, these data are consistent with previous reports that BN 52021 inhibits PAF degradation under nonapoptotic culture conditions (48, 50). PAF-AH I α_2/α_2 is known to hydrolyze PAF more efficiently than α_1/α_1 homodimers, and it is likely that reducing PAF-AH α_1 coincident with PAF-AH α_2 induction would promote more rapid formation of α_2/α_2 homodimers, enhance PAF hydrolysis, and increase cell survival. Most interestingly, this phenomenon models the graded reduction in α_1 observed over the course of cerebral development by changing the predominant PAF-AH I catalytic composition from α_1/α_2 heterodimers in embryonic central nervous system to α_2/α_2 homodimers in adult brain (51). Our data suggest that this shift may render adult brain more resistant to PAF challenge than embryonic brain.

Summary—In summary, this study provides mechanistic evidence that sustained exposure to elevated intracellular PAF concentrations is sufficient to elicit apoptosis through a PAFR-independent cell death pathway. Previous studies have demonstrated that oxidative modification of membrane lipids during atherosclerotic injury, treatment with chemotherapeutic agents, ultraviolet B exposure, or excitoxicity is sufficient to produce PAF-like lipids (6, 19, 30, 31, 40). Our data suggest that these effects can occur in the absence of PAFR. To intervene in PAF-mediated death, we describe a novel anti-apoptotic function for PAF-AH I α_2 and II, and we identify two PAF antagonists that accelerate cytosolic PAF-AH I activity to inhibit PAF-mediated apoptosis.

Acknowledgments—We thank Tia Moffat for technical assistance and Jim Bennett for critical reading of this manuscript.

REFERENCES

1. Birkle, D. L., Kurian, P., Braquet, P., and Bazan, N. G. (1998) *J. Neurochem.* **51**, 1900–1905
2. Bazan, N. G. (1998) *Prog. Brain Res.* **118**, 281–291
3. Perry, S. W., Hamilton, J. A., Tjoelker, L. W., Dbaibo, G., Dzenko, K. A., Epstein, L. G., Hannun, Y., Whittaker, J. S., Dewhurst, S., and Gelbard, H. A. (1998) *J. Biol. Chem.* **273**, 17660–17664
4. Bate, C., Reid, S., and Williams, A. (2004) *J. Biol. Chem.* **279**, 36405–36411
5. Bate, C., Salmona, M., and Williams, A. (2004) *Neuroreport* **15**, 509–513
6. Li, T., Southall, M. D., Yi, Q., Pei, Y., Lewis, D., Al-Hassani, M., Spandau, D., and Travers, J. B. (2003) *J. Biol. Chem.* **278**, 16614–16621
7. Darst, M., Al-Hassani, M., Li, T., Yi, Q., Travers, J. M., Lewis, D. A., and Travers, J. B. (2004) *J. Immunol.* **172**, 6330–6335
8. Fukuda, Y., Kawashima, H., Saito, K., Inomata, N., Matsui, M., and Nakanishi, T. (2000) *Eur. J. Pharmacol.* **390**, 203–207

9. Grandel, K. E., Farr, R. S., Wanderer, A. A., Eisenstadt, T. C., and Wasserman, S. I. (1985) *N. Engl. J. Med.* **313,** 405–409
10. Ishii, S., and Shimizu, T. (2000) *Prog. Lipid Res.* **39,** 41–82
11. Brewer, C., Bonin, F., Bullock, B., Nault, M.-C., Morin, J., Imbeault, S., Shen, T. Y., Franks, D. J., and Bennett, S. A. L. (2002) *J. Neurochem.* **18,** 1502–1511
12. Southall, M. D., Isenberg, J. S., Nakahatri, H., Yi, Q., Pei, Y., Spandau, D. F., and Travers, J. B. (2001) *J. Biol. Chem.* **276,** 45548–45554
13. Tokuoka, S. M., Ishii, S., Kawamura, N., Satoh, M., Shimada, A., Sasaki, S., Hirotsune, S., Wynshaw-Boris, A., and Shimizu, T. (2003) *Eur. J. Neurosci.* **18,** 563–570
14. Bratton, D. L. (1993) *J. Biol. Chem.* **268,** 3364–3373
15. Bratton, D. L., Dreyer, E., Kailey, J. M., Fadok, V. A., Clay, K. L., and Henson, P. M. (1992) *J. Immunol.* **148,** 514–523
16. Sapir, T., Elbaum, M., and Reiner, O. (1997) *EMBO J.* **16,** 6977–6984
17. Marcheselli, V. L., Rossowska, M., Domingo, M. T., Braquet, P., and Bazan, N. G. (1990) *J. Biol. Chem.* **265,** 9140–9145
18. Hostettler, M. E., Knapp, P. E., and Carlson, S. L. (2002) *Glia* **38,** 228–239
19. Ma, X., and Bazan, H. E. P. (2001) *Curr. Eye Res.* **23,** 326–335
20. Tong, N., Sanchez, J. F., Maggirwar, S. B., Ramierez, S. H., Guo, H., Dewhurst, S., and Gelbard, H. A. (2001) *Eur. J. Neurosci.* **13,** 1913–1922
21. Manya, H., Aoki, J., Kato, H., Ishii, J., Hino, S., Arai, H., and Inoue, K. (1999) *J. Biol. Chem.* **274,** 31827–31832
22. Hattori, M., Adachi, H., Tsujimoto, M., Arai, H., and Inoue, K. (1994) *Nature* **370,** 216–218
23. Hattori, K., Adachi, H., Matsuzawa, A., Yamamoto, K., Tsujimoto, M., Aoki, J., Hattori, M., Arai, H., and Inoue, K. (1996) *J. Biol. Chem.* **271,** 33032–33038
24. Min, J.-H., Wilder, C., Aoki, J., Arai, H., Inoue, K., Paul, L., and Gelb, M. H. (2001) *Biochemistry* **40,** 4539–4549
25. Matsuzawa, A., Hattori, K., Aoki, J., Arai, H., and Inoue, K. (1997) *J. Biol. Chem.* **272,** 32315–32320
26. Marques, M., Pei, Y., Southall, M. D., Johnston, J. M., Arai, H., Aoki, J., Inoue, T., Seltmann, H., Zouboulis, C. C., and Travers, J. B. (2002) *J. Investig. Dermatol.* **119,** 913–919
27. Tjoelker, L. W., Eberhardt, C., Unger, J., Trong, H. L., Zimmerman, G. A., McIntyre, T. M., Stafforini, D. M., Prescott, S. M., and Gray, P. W. (1995) *J. Biol. Chem.* **270,** 25481–25487
28. Asano, K., Okamoto, S., Fukunaga, K., Shiomi, T., Mori, T., Iwata, M., Ikeda, Y., and Yamaguchi, K. (1999) *Biochem. Biophys. Res. Commun.* **261,** 511–514
29. Hirashima, Y., Ueno, H., Karasawa, K., Yokoyma, K., Setaka, M., and Takaku, A. (2000) *Brain Res.* **885,** 128–132
30. Ogden, F., DeCoster, M. A., and Bazan, N. G. (1998) *J. Neurosci. Res.* **15,** 677–684
31. Chen, C. H., Jiang, T., Yang, J. H., Jiang, W., Lu, J., Marathe, G. K., Pownall, H. J., Ballantyne, C. M., McIntyre, T. M., Henry, P. D., and Yang, C. Y. (2003) *Circulation* **107,** 2102–2108
32. Bligh, E. C., and Dyer, W. J. (1959) *Can. J. Biochem.* **37,** 911–917
33. Bennett, S. A. L., Chen, J., Pappas, B. A., Roberts, D. C. S., and Tenniswood, M. (1998) *Cell Death Differ.* **5,** 867–875
34. O'Flaherty, J., Redman, J., Schmitt, J., Ellis, J., Surles, J., Marx, M., Piantadosi, C., and Wykle, R. (1987) *Biochem. Biophys. Res. Commun.* **147,** 18–24
35. Hattori, K., Hattori, M., Adachi, H., Tsujimoto, M., Arai, H., and Inoue, K. (1995) *J. Biol. Chem.* **270,** 22308–22313
36. Ohshima, N., Ishii, S., Izumi, T., and Shimizu, T. (2002) *J. Biol. Chem.* **277,** 9722–9727
37. Pietri, S., Maurelli, E., Drieu, K., and Culcasi, M. (1997) *J. Mol. Cell. Cardiol.* **29,** 733–742
38. Yoshida, K., Okamoto, M., Shimazaki, N., and Hemmi, K. (1988) *Prog. Biochem. Pharmacol.* **22,** 66–80
39. Okamoto, M., Yoshida, K., Uchida, I., Kohsaka, M., and Aoki, H. (1986) *Chem. Pharm. Bull.* **34,** 345–348
40. Barber, L. A., Spandau, D. F., Rathman, S. C., Murphy, R. C., Johnson, C. A., Kelley, S. W., Hurwitz, S. A., and Travers, J. B. (1998) *J. Biol. Chem.* **273,** 18891–18897
41. Lu, J., Caplan, M. S., Saraf, A. P., Li, D., Adler, L., Liu, X., and Jilling, T. (2004) *Am. J. Physiol.* **286,** G340-G350
42. Mori, M., Aihara, M., Kume, K., Hamanoue, M., Kohsaka, S., and Shimizu, T. (1996) *J. Neurosci.* **16,** 3590–3600
43. Kornecki, E., and Ehrlich, Y. H. (1988) *Science* **240,** 1792–1794
44. Terashita, Z., Imura, Y., Takatani, M., Tsushima, S., and Nishikawa, K. (1987) *J. Pharmacol. Exp. Ther.* **242,** 263–268
45. Valone, F. H. (1985) *Biochem. Biophys. Res. Commun.* **126,** 502–508
46. Nunez, D., Chignard, M., Korth, R., Le Couedic, J. P., Norel, X., Spinnewyn, B., Braqueit, P., and Benveniste, J. (1986) *Eur. J. Pharmacol.* **123,** 197–205
47. Dupré, D. J., Le Gouill, C., Rola-Pleszczynski, M., and Stanková, J. (2001) *J. Pharmacol. Exp. Ther.* **2999,** 358–365
48. Lachachi, H., Plantavid, M., Simon, M. F., Chap, H., Braquet, P., and Douste-Blazy, L. (1985) *Biochem. Biophys. Res. Commun.* **132,** 460–466
49. Gerard, N. P., and Gerard, C. (1994) *J. Immunol.* **152,** 793–800
50. Lamant, V., Mauco, G., Braquet, P., Chap, H., and Douste-Blazy, L. (1987) *Biochem. Pharmacol.* **36,** 2749–2752
51. Manya, H., Aoki, J., Watanabe, M., Adachi, T., Asou, H., Inoue, Y., Arai, H., and Inoue, K. (1998) *J. Biol. Chem.* **273,** 18567–18572

Was the Ataxia of Pierre Marie Machado-Joseph Disease?

A Reappraisal Based on the Last Autopsy Case From la Salpêtrière Hospital

Toshiki Uchihara, MD, PhD; Charles Duyckaerts, MD, PhD; Kiyoshi Iwabuchi, MD, PhD; Makoto Iwata, MD, PhD; Saburo Yagishita, MD, PhD; Jean-Jacques Hauw, MD, PhD

Nosological placement of *l'hérédo-ataxie cérébelleuse de Pierre Marie* (HAC) has never been established even after several autopsy cases from the original Haudebourg family had been reported. To reappraise the clinical and pathological features of HAC in the current framework of hereditary ataxias, we screened the autopsy records of la Salpêtrière hospital and identified a patient with a diagnosis of HAC who underwent an autopsy in 1943. Clinical features included heredity compatible with autosomal dominant inheritance, spasticity, increased tendon reflexes, mask-like face, visual impairment, nuclear ophthalmoparesis, and exophthalmos in addition to progressive ataxia. Pathological lesions included the spinal cord (spinocerebellar tracts, anterolateral fascicles, and posterior column), cerebellar dentate nucleus, pontine nucleus, pallidum, motor neurons including the oculomotor nucleus, and substantia nigra. The cerebellar cortex and inferior olives were preserved. These clinical and pathological features, similar to those described in patients from the Haudebourg family, a core prototype of HAC, are indistinguishable from those of Machado-Joseph disease. It would then be possible to conclude that some of the patients historically considered to have HAC would today be classified as having Machado-Joseph disease.

Arch Neurol. 2004;61:784-790

Pierre Marie, professor and head of the department of Neurology at Paris Medical School, proposed the concept of *l'hérédo-ataxie cérébelleuse* (HAC) in 1893.[1] Its precise definition, however, remains to be established,[2] because this proposal by Pierre Marie was mainly based on clinical findings with special reference to retained or exaggerated tendon reflexes[3,4] and 2 previous pathological studies,[5,6] both reporting lesions distinct from those seen in Friedreich ataxia.[7] Classification of hereditary ataxias has thereafter been confronted with difficulties because the nosological framework could not be established on a firm basis. The data presented in subsequent autopsy reports[8-11] on the affected members of the Haudebourg family, clinically described by Klippel and Durante,[3] have been considered prototypic of HAC. The current nosological position of Pierre Marie hereditary ataxia remains to be determined; one may wonder how the original cases should be classified now that the diagnosis relies on a firm genetic ground. After the last patient from the Haudebourg family was reported in 1941 by Guillain et al,[11] however, the term *HAC* has been rarely mentioned in the literature and in clinical practice.[12-15] Its nosological identity became more and more obscured and possibly has been confounded with various hereditary ataxias with retained or exaggerated tendon reflexes (other than Friedreich ataxia).

We have tried to determine to which present day diagnosis HAC could corre-

From the Laboratoire Raymond Escourolle, Service de Neuropathologie, Association Claude Bernard, Groupe Hospitalier, Pitié-Salpêtrière, Paris, France (Drs Uchihara, Duyckaerts, and Hauw); the Department of Neuropathology, Tokyo Metropolitan Institute for Neuroscience, Tokyo, Japan (Dr Uchihara); the Departments of Neurology and Psychiatry (Dr Iwabuchi) and Pathology (Dr Yagishita), Kanagawa Rehabilitation Center, Kanagawa, Japan; and the Department of Neurology, Tokyo Women's Medical University, Tokyo (Dr Iwata).

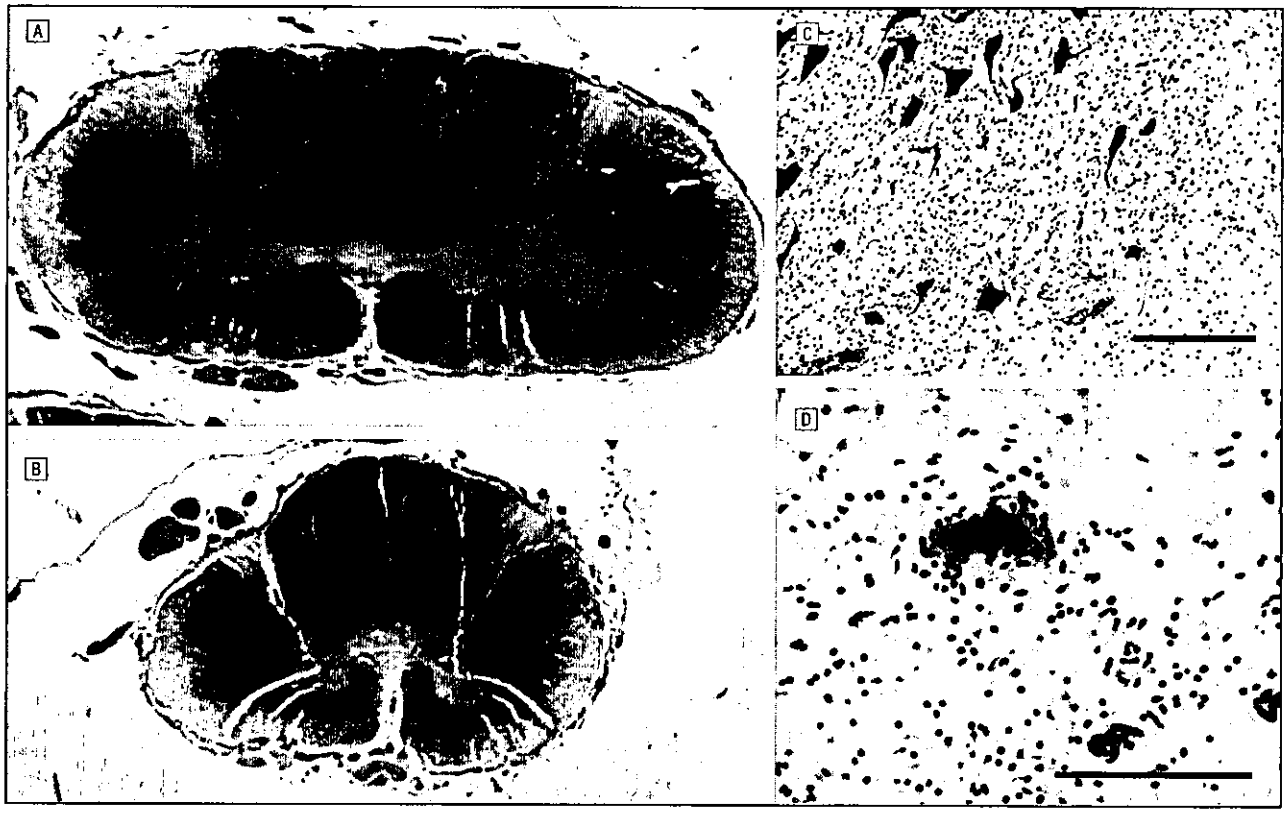

Figure 1. Present-day photographs of original slides. Macroscopic and microscopic changes of the spinal cord. A, Lower cervical cord (myelin). Anterior and posterior spinocerebellar tracts are involved bilaterally. Atrophy in the anterior horn and a slight pallor in the posterior column are present. B, Middle thoracic cord (myelin). Anterior and posterior spinocerebellar tracts are involved. The lesion extends deeper into anterolateral portion of the spinal cord. C, Anterior horn of the lumbar cord (Nissl). Massive gliosis and neuronal atrophy are observed in the anterior horn (scale bar, 200 μm). D, Clarke column (Nissl). No neuronal cells are identifiable in the Clarke column (scale bar, 100 μm).

spond. We think that this inquiry might have some utility because descendents of patients with HAC are probably still alive, receiving diagnoses and being cared for. This prompted us to screen the autopsy records of la Salpêtrière hospital to look for patients with the diagnosis of HAC. After the last report by Guillain et al,[11] only a single case was labeled with this diagnosis. Retrospective analysis of the clinicopathological features of this patient, identical to those exhibited by patients from the original Haudebourg family, revealed that the features were also compatible with those of Machado-Joseph disease (MJD).

The autopsy record (autopsy number 1541, October 15, 1943) was accompanied by 5 handwritten pages describing the clinical history and the neurological examination. This is, verbatim, their translation:

His mother presented with similar neurological features at the age of 38 with gait and speech disturbance. She died at the age of 58 at the hospice for patients with incurable diseases at Ivry. She had a daughter (of her first marriage), who was affected by the same disease.

Among children of her second marriage, two (were affected), this patient and his brother, who is 33 years old and has a difficulty in speaking. His voice is similar to that of her brother and of her sister, but he could not be examined.

This patient is admitted for:

- Difficulty in speech. Traceable to his early childhood. Slowed and slurred speech, which became progressively marked.
- Gait disturbances. They appeared at the age of 34, he swayed and hardly went up the stairs. In 1937, had to use 2 walking sticks. Numbness of the arms appeared at the same time.
- Visual difficulties: His visual acuity declined when motor deficits became apparent. He could not see well. He had the feeling of looking through a curtain. In 1938, he left his job.

Examination. Gait: He walks with difficulty. The legs are rigid and extended, gait with short steps, wide based. Movements are spastic. During walking, the head is unstable with slow swaying in anterior-posterior direction. No progression after April, 1940. Muscle tone is a little increased. Muscle strength is conserved.

Reflexes: Deep tendon reflexes are increased. Even markedly exaggerated bilaterally at patella and Achilles. Contralateral reflexes of adductors are extensive. Upper extremities: reflexes exaggerated and symmetric. Plantar reflex in flexion, defensive movement being triggered by the stimulation. Cremasteric reflexes normal at the right side, not regularly obtained at the left side. Although abdominal cutaneous reflexes are conserved only in the upper abdomen, it is weak. Clonus. Sensibility: normal.

Cerebellar signs: Marked dysmetria on four extremities. Adiadochokinesis. Speech is slowed and slurred. No intension tremor. No nystagmus. No trophic changes. No disturbances of sphincters. No extrapyramidal signs, except for expressionless face.

Cranial nerves: I: normal, II: Nerve atrophy on funduscopic examination, suggesting myopic staphyloma, III, IV, VI: bilateral paresis of the superior rectus. Other extraocular muscles are also paretic except for probably the inferior

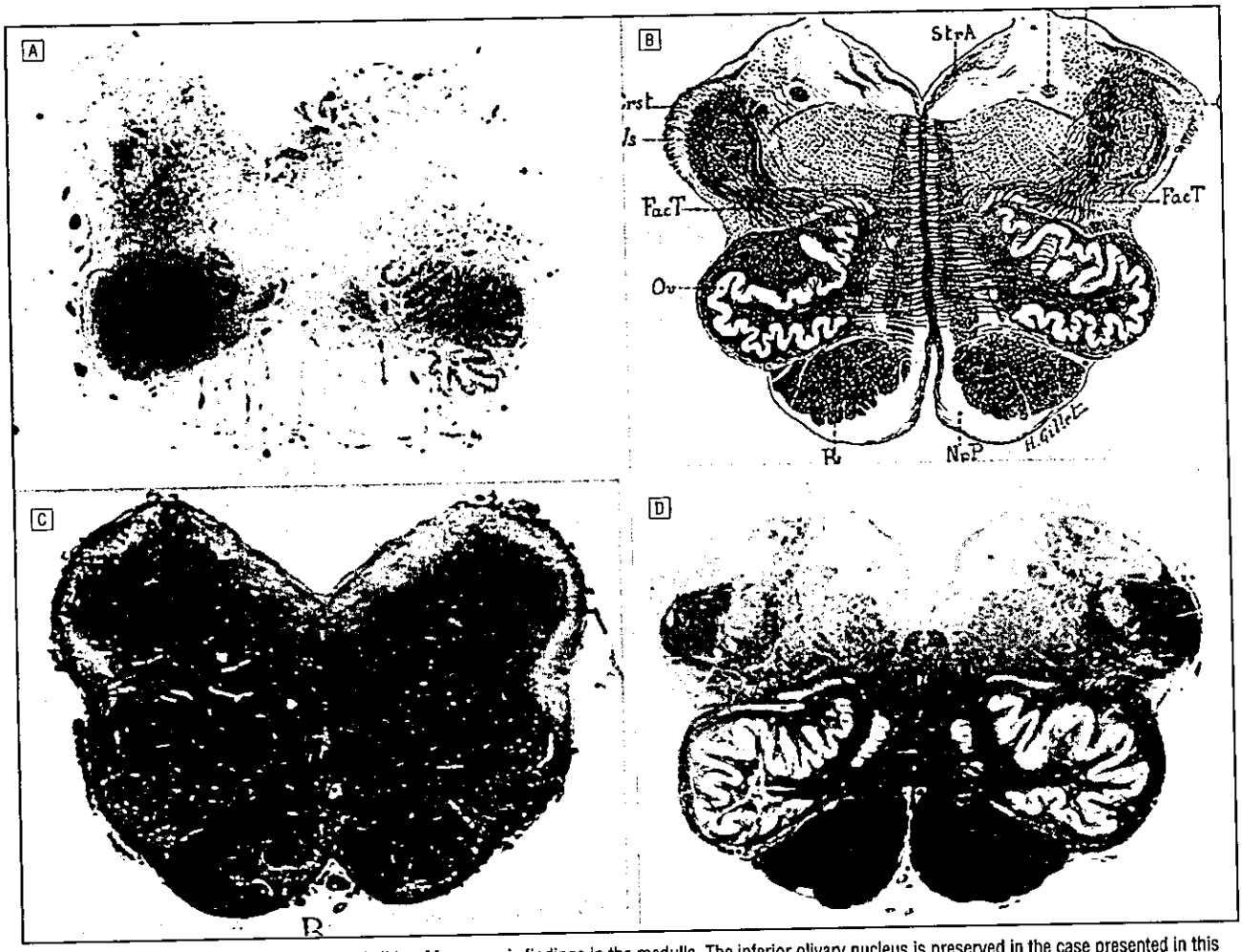

Figure 2. Present-day photographs of original slides. Macroscopic findings in the medulla. The inferior olivary nucleus is preserved in the case presented in this study (A) and patients from the Haudebourg family (B, Amélie Haudebourg, citation 10) (C, François Haudebourg, citation 9). This holds true in patients with typical Machado-Joseph disease (D).

rectus. Bilateral exophthalmos. Light reflex is detectable and very slight. VII: No facial weakness. Mask-like face. VIII: Auditory acuity normal, but, on both sides, central deficit of vestibular nerves with inexcitability. IX, X, XI, XII: Normal.

On August 3, 1943, large bilateral cavities, (on August) 15, died.

Clinical diagnosis. Hérédoataxie de Pierre Marie.

An autopsy was performed on the same day. The neuropathological report (1571), which was not signed but was probably written by Yvan Bertrand, who was in charge of the laboratory, indicated:

Marked atrophy of the brainstem, moderate atrophy of the cerebellum. Nothing particular at the level of the cerebrum. Spinal cord [**Figure 1**A and B], Very badly sampled, damaged by hammer and knife. Aspect of the spinal cord not very characteristic of hérédoataxie; sclerosis of anterolateral tracts and marginal tracts, however, can be identified [Figure 1A and B]. High cervical section: spongiosis in the dorsal column [Figure 1A].

Medulla [**Figure 2**A], damaged at autopsy. Not so atrophic relatively. Pyramids intact. Pallor of the fibers around the olives. Spongiosis of the restiform body, very atrophied. Atrophy of the solitary fascicle. Acoustic striae untouched.

Mesocephalon (=mesencephalon): Generalized atrophy, but especially remarkable in the tegmentum, where demyelination is severely advanced. On the other hand, stretching and V-shaped distortion. Medial longitudinal fasciculus: normal. Crus cerebri: normal. Sclerosis of the spinocerebellar tract is present but not massive. This moderate change is in contrast with diffuse atrophy of the brainstem without system selectivity.

Pons [**Figure 3**A and B]: equally very atrophic, pallor of the tegmentum and of several transverse pontocerebellar bundles (reduction in number rather than degeneration). Pyramidal tract untouched. Near the median line in the base of the pons, a site of prelacunar, hemorrhagic and spongy state. The cerebellar white matter is compact except in its posterior and upper portions, where subcortical rarefaction is present, a kind of prelacunar state. The dentate nucleus [Figure 3A], very atrophic, evident lesion: cell loss, liquefaction, glial infiltration and pallor of the fibers around the nucleus [Figure 3C]. This entire region is very fragile. The origin of the superior cerebellar peduncle is severely rarefied and atrophied.

Cerebellum [Figure 3D]: Laminar atrophy of moderate degree with reduction in the number of the various constituents: granule cells and Purkinje cells. As a whole, however, one has the feeling of laminar primary cortical atrophy with secondary degeneration of the centers of the brainstem.

In the cerebellum and brainstem, the atrophy is more severe than the degeneration of selected systems. The sparing of the pyramidal tract, and the spinocerebellar tract involvement authorizes the diagnosis of "hérédo-ataxie" despite the absence of ventral predominance of the lesions.